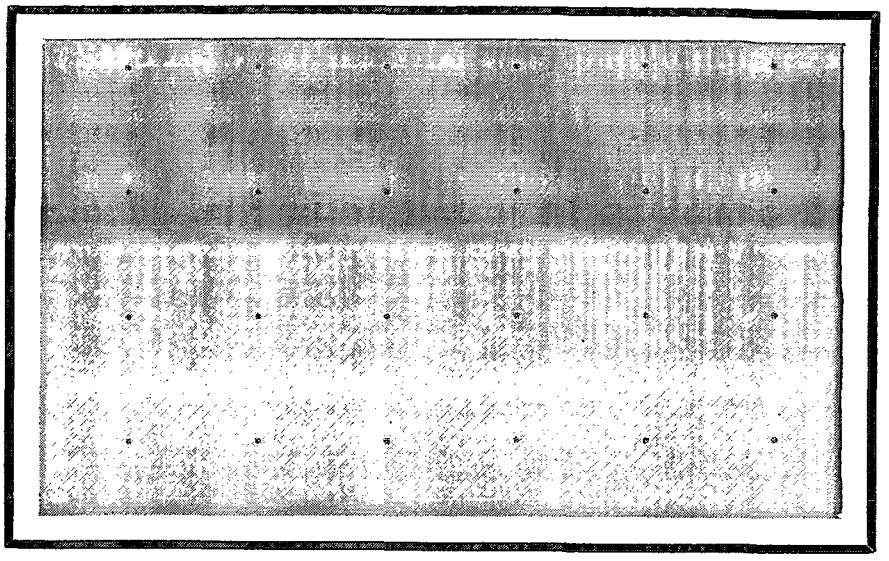

MICROWAVE DEVICE AND PHYSICAL
ELECTRONICS LABORATORY
DEPARTMENT OF ELECTRICAL ENGINEERING

UNIVERSITY OF UTAH
SALT LAKE CITY, UTAH 84112

University of Utah
Research Committee

UTEC MD 71-061

AMPLITUDE AND POLARIZATION ASYMMETRIES IN A RING LASER

by

L. L. Campbell and N. E. Buholz

Technical Report RC-1

January 1971

Microwave Device and Physical Electronics Laboratory
Electrical Engineering Department
University of Utah
Salt Lake City, Utah

ABSTRACT

Asymmetric amplitude effects between the oppositely directed traveling waves in a He-Ne ring laser are analyzed both theoretically and experimentally. These effects make it possible to detect angular orientations of an inner-cavity bar with respect to the plane of the ring cavity. The amplitude asymmetries occur when a birefringent bar is placed in the three-mirror ring cavity, and an axial magnetic field is applied to the active medium.

The theoretical problem is complicated by the presence of axial magnetic field effects in the active medium, anisotropic loss resulting from the Brewster windows, and linear birefringence exhibited by the quartz bar. A simplified theoretical analysis is performed by using a first order perturbation theory to derive an expression for the polarization of the active medium, and a set of self-consistent equations are derived to predict threshold conditions. It is determined that the amplitude asymmetries are caused by the axial magnetic field effects in the active medium and the linear birefringence of the bar. Polarization asymmetries between the oppositely directed waves are also predicted. The amplitude and polarization asymmetries are only predicted to occur in cavities formed by an odd number of mirrors (in this case, three).

Amplitude asymmetries similar in nature to those predicted at threshold occur when the laser is operating in 12-15 free-running modes. These asymmetries also exist at power levels near threshold.

The polarization asymmetry occurs simultaneously with the amplitude asymmetries. Both amplitude and polarization asymmetries cease to exist in a four-mirror cavity. Asymmetric polarization changes are shown to occur between oppositely directed waves when light on a single-pass propagates through the combination of an active medium in the presence of an axial magnetic field and a birefringent bar in a three-mirror cavity.

The percent increase or decrease in the intensity of the oppositely directed waves is found to be approximately linear for small rotations of the quartz bar, thus making it easy to determine the angular orientation of the bar by monitoring the magnitude and sign of the oppositely directed wave intensities.

ACKNOWLEDGMENT

The authors express their appreciation to the Research Committee of the University of Utah for their support of the research project described in this report, and to the National Aeronautics and Space Administration for Mr. Campbell's Graduate Fellowship.

TABLE OF CONTENTS

LIST OF ILLUSTRATIONS AND TABLES

PREFACE

A ring laser is a device in which the mirrors forming the laser cavity are placed at the corners of a polygon. Active material is placed along one or more sides of the polygon. Laser action occurs for waves which are resonant in the polygon and which have sufficient gain in the active medium. Such waves have a gain equal loss condition around the ring and continue to circulate indefinitely.

The important difference between ring lasers and other lasers is that the normal modes of the ring are traveling waves rather than standing waves. Hence, it is possible to obtain two waves traveling in opposite directions around the ring which do not have the same amplitude or frequency even though they are associated with the same resonant frequency of the polygon. The two amplitudes differ if the waves see different gain or loss as they traverse the ring perimeter, and the two frequencies differ if the optical path length is different in the two directions. Thus the ring laser provides a means by which phenomena that result in either a gain/loss or refractive nonreciprocity may be studied and utilized.

Most attention has been directed toward studies involving refractive nonreciprocity. Frequency differences caused by the Doppler shift between the oppositely directed waves have been used

to detect rotation rates.[1,2] Refractive nonreciprocity has also been used in other applications such as in the measurement of gas flow profiles.[3]

For a single oscillating mode in each direction, Aronowitz[4] has shown theoretically that the amplitudes of the oppositely directed (OD) waves change differently when the oscillating frequency of the two modes are sufficiently close to each other to cause gain competition effects in the active medium. His predictions were verified experimentally by Hutchings, et al.[5] Lee and Atwood[6] have experimentally shown that if the single oscillating mode of one direction is separated in frequency far enough from the single oscil-

---

[1] W. M. Macek, D. T. M. Davis, Jr., R. W. Olthuis, J. R. Schneider, and G. R. White, "Ring Laser Rotation Rate Sensor," presented at the Symposium on Optical Masers, Polytechnic Institute of Brooklyn, Brooklyn, New York, April 16-19, 1963.

[2] E. O. Schulz and DuBois, "Alternative Interpretation of Rotation Rate Sensing by a Ring Laser," *IEEE Journal of Quantum Electronics*, Vol. QE-2, No. 8, August 1966, pp. 299-305.

[3] P. Fenster and W. K. Kahn, "An Optical Technique for Measurement of Gas Flow Profiles Utilizing a Ring Laser," *Applied Optics*, Vol. 7, No. 12, December 1968, pp. 2383-2390.

[4] F. Aronowitz, "Theory of a Traveling-Wave Optical Maser," *Physical Review*, Vol. 139, No. 3a, August 1965, pp. A635-A646.

[5] T. J. Hutchings, J. Winocur, R. H. Durrett, E. D. Jacobs, and W. L. Zingery, "Amplitude and Frequency Characteristics of a Ring Laser," *Physical Review*, Vol. 152, No. 1, December 1966, pp. 467-473.

[6] P. H. Lee and J. G. Atwood, "Measurement of Saturation Induced Optical Nonreciprocity in a Ring Laser Plasma," *IEEE Journal of Quantum Electronics*, Vol. QE-2, No. 8, August 1966, pp. 235-243.

lating mode of the opposite direction to prohibit gain competition effects, then the amplitudes of the OD waves can be varied differently by providing a loss asymmetry between the two waves.

We have found that asymmetric amplitude changes can be induced between the OD waves in a ring laser operating in 12-15 free-running modes. These asymmetries occur when a birefringent bar is placed in a three-mirror ring cavity and an axial magnetic field is applied to the active medium. The amplitude changes have the following characteristics. The birefringent bar is placed in the cavity as shown in Fig. 1. When a static axial magnetic field is applied to the active medium, at certain bar orientations, the average intensity of one wave increases while the average intensity of the OD wave decreases. As the bar is rotated to another orientation, we find that upon applying the field, the wave which increased in intensity before now decreases in intensity while the OD wave's intensity increases.

It is apparent that the asymmetric effect results from unequal changes in the gain/loss ratio of the OD waves, where the term "gain" here refers to the unsaturated gain. The gain/loss ratio is determined, in part, by the polarization of these waves. We find experimentally that, as the asymmetries occur, the net polarization of one set of waves changes differently from that of the OD set. That is, a polarization asymmetry is found to occur simultaneously with the amplitude asymmetry.

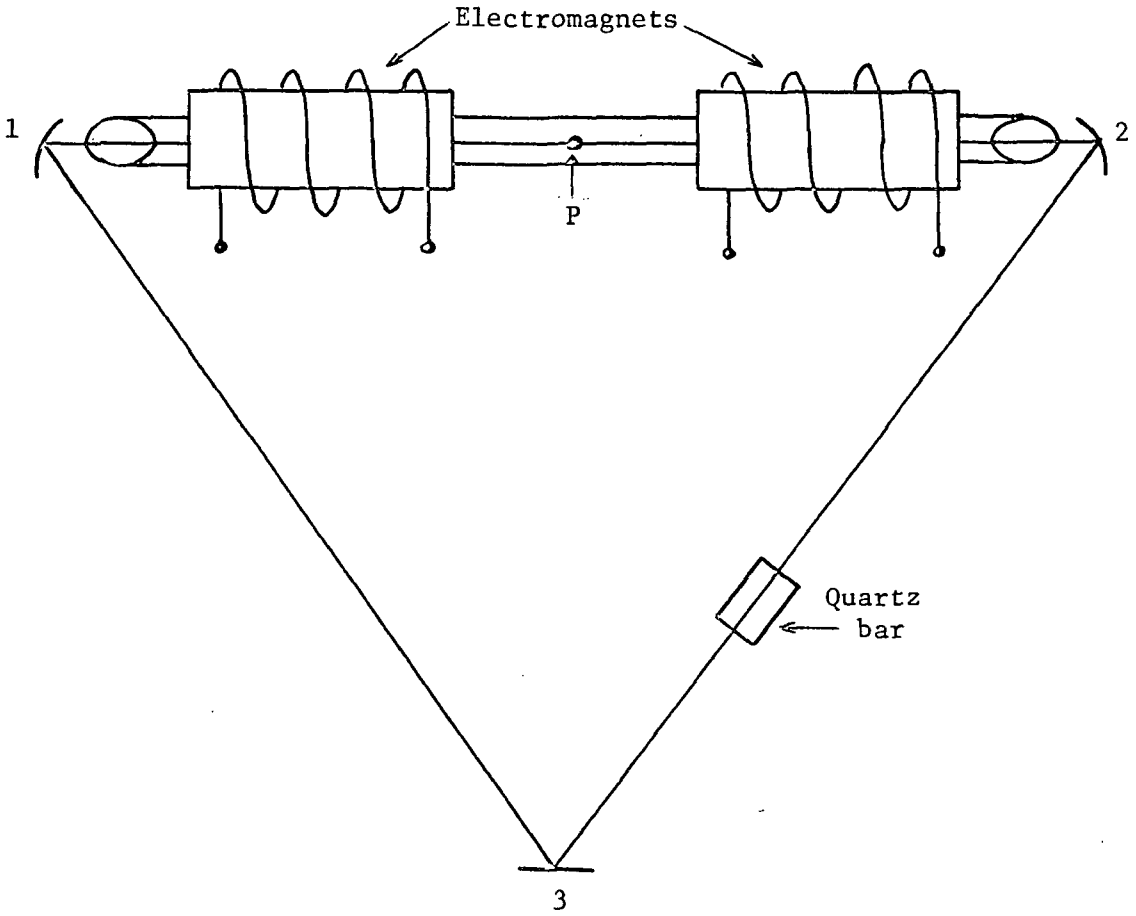

Fig. 1. Ring laser schematic.

The polarization of the waves in the ring laser is determined by several factors -- the Brewster windows, resonance conditions of the empty three-mirror cavity, the quartz bar, and the magnetic field effects upon the gain atoms. The Brewster windows on the plasma tube have a minimum reflection loss for only one linear polarization. As will be shown, a three-mirror ring laser, as illustrated in Fig. 1 but without internal cavity birefringence or magnetic field effects, can only support waves with two polarizations -- one linearly polarized normal to the plane of the ring, the other linearly polarized in the plane of the ring.[7] The quartz bar, like the Brewster windows, has a minimum reflection loss for only one polarization. Another property of the bar is its birefringence which in general causes the polarization of light passing through it to be changed.

Besides the quartz bar, when an axial magnetic field is applied to the active medium, there are additional polarization effects.[8-11]

---

[7] S. N. Bagaev, Y. V. Troitskii and B. I. Troshin, "The Polarization of Radiation and the Frequency Characteristics of Ring Lasers with a Triangular Resonator," *Optics and Spectroscopy*, Vol. 21, No. 6, December 1966, pp. 420-421.

[8] M. Sargent, III, W. E. Lamb, Jr., and R. L. Fork, "Theory of a Zeeman Laser, I and II," *Physical Review*, Vol. 164, No. 2, December 16, 1967, pp. 436-465.

[9] R. G. Buser, J. Kainz and J. Sullivan, "Influence of Magnetic Fields upon Gas Discharge Lasers," *Applied Optics*, Vol. 2, No. 8, August 1963, pp. 861-862.

[10] C. V. Heer and R. D. Graft, "Theory of Magnetic Effects in Optical Maser Amplifiers and Oscillators," *Physical Review*, Vol. 140, No. 4A, November 15, 1965, pp. A1088-A1104.

[11] G. J. Burrell, A. Hetherington and T. S. Moss, "Faraday Rotation Resulting from Negative Absorption," *Proceedings of the Physical Society*, Vol. 1, Ser. 2, 1968, pp. 692-696.

These effects arise because the active atoms in the region of the axial magnetic field have Zeeman-shifted energy levels or transition frequencies, and they only interact with right- or left-hand circularly polarized light. When a linearly polarized wave, which can be resolved into a right- and left-hand circularly polarized wave encounters such a system, it interacts with some atoms associated with right-hand circular polarization and some associated with left-hand circular polarization. In general, there is a different number of atoms in each group, and hence the polarization of the wave as it emerges from the region of the magnetic field is elliptical with major axis rotated from what it was when it entered.

It will be the subject of this work to understand the source of the amplitude asymmetries, and how they are influenced by the above polarization sensitive effects. The basis for the study of these asymmetric effects is their possible utilization to detect angular orientations of an inner-cavity element with respect to the ring cavity.

Two different types of theoretical analysis can be applied to the problem. The first involves the matrix method introduced by Jones[12] in which each element of the cavity is represented by a transmission matrix. The resultant matrix found by multiplying the

---

[12] R. C. Jones, et al., *Journal of the Optical Society of America*, Vol. 31, No. 7, 1941, pp. 488-503; Vol. 32, No. 8, 1942, pp. 486-493; Vol. 37, No. 2, 1947, pp. 107-112; Vol. 38, No. 2, 1948, pp. 671-685; Vol. 46, No. 2, 1956, pp. 126-131.

transmission matrices together is used to derive the eigenstates of the polarization in the system.[13] To use this method one must obtain a transmission matrix describing the active medium which appears to be a difficult problem. The second method, and the one we will use, is to follow Lamb's treatment of the optical maser oscillator.[14] Aronowitz[15] used this approach to discuss the ring laser oscillator; however, he did not include magnetic field effects in the active medium, loss anisotropy, or birefringence. Sargent, et al.,[16] included these effects in a standing wave laser. We will include the effects of a magnetic field, loss anisotropy, and birefringence in the description of a ring laser oscillator.

As in Lamb's[17] semiclassical treatment, we assume a classical electromagnetic field exists in the cavity. This field acts on the active medium, which is composed of atoms described by quantum mechanical laws, causing the medium to become polarized. The resulting macroscopic polarization then acts as a source for the electromagnetic field according to Maxwell's equations. We then require the

---

[13] H. deLang, "Eigenstates of Polarization in Lasers," Philip Research Reports, Vol. 19, 1964, pp. 429-440.

[14] W. E. Lamb, Jr., "Theory of an Optical Maser," *Physical Review*, Vol. 134, No. 6a, June 1964, pp. A1429-A1450.

[15] F. Aronowitz, *op. cit.*

[16] M. Sargent, III, et al., *op. cit.*

[17] W. E. Lamb, Jr., *op. cit.*

field assumed in the cavity to be self-consistent with the field produced.

The macroscopic polarization can be derived from the equations of motion of the density operator in which the electric field is a perturbation term. The atoms in the active medium are Doppler shifted because of their thermal velocity. Therefore, atoms with different velocities resonate with different frequencies. Consequently, we cannot obtain an exact solution to the equations of motion. Therefore, an iterative type solution, using a perturbation expansion in powers of the electric field, is performed. Terms which contribute to the macroscopic polarization are obtained in first, third, etc., orders. As Lamb shows many nonlinear effects are obtained in the third order. However, when one adds in the complexities of magnetic field effects, anisotropic loss, and birefringence, the problem becomes sufficiently complex that it would be difficult to draw meaningful conclusions from the equations, let alone the formidable problem of solving the equations. We, therefore, use the first order theory to derive an expression for the polarization of the active medium. The polarization is then used in the self-consistent equations to obtain a set of four coupled equations describing each propagation direction. These equations are used to draw conclusions as to the cause of the aforementioned amplitude asymmetries.

It is important to note that this theory, being a first order theory, can predict threshold conditions; however, interactions such

as competition between modes of the same direction, between modes of the opposite direction and saturation effects will not be predicted. We are lead to attempt the first order theory due to its simplicity and because we find the amplitude asymmetries also occur near threshold.

In chapter I a theoretical description of the multimode ring laser, including magnetic field effects, loss anisotropy, and linear birefringence, is developed. The axial magnetic field effects in the active medium are included in the manner presented by Sargent, et al.[18] A constitutive conductivity tensor "σ" is included in the wave equation to account for loss anisotropy and birefringence. The implications of the theory are discussed.

Experimental results are presented in chapter II. The characteristics of the amplitude asymmetry and associated polarization asymmetry are explained. The results of various experiments are illustrated indicating how the amplitude asymmetries vary as a function of bar orientation. The results of related experiments are presented and their meaning is discussed. A conclusions section is presented in chapter III in which specific experimental results are correlated with theoretical predictions.

---

[18] M. Sargent, III, et al., *op. cit.*

I. THEORY OF THE RING LASER

1.1. Introduction

In this chapter we apply Lamb's[19] semiclassical treatment of the optical maser oscillator to the traveling wave case to develop a theoretical model of the multimode ring laser. The effects of a static axial magnetic field in the active medium region, Brewster window loss, and cavity birefringence are included.

As in Bahr's[20] analysis of the internally modulated ring laser, a traveling wave description of the electric field is used to derive a set of "circuit" equations in the amplitudes and phases of the n^{th} mode for each polarization component and in each propagation direction. The presence of anisotropic loss, birefringence, and magnetic field effects complicate the problem by forcing the oppositely directed (OD) traveling waves to be elliptically polarized. The anisotropic loss and birefringence are introduced phenomenologically into the wave equation through respective conductivity and susceptibility tensors.

The action of a birefringent bar on the OD traveling waves is described by a transfer function. This function is developed for each propagation direction in the three-mirror ring cavity. It is then used to obtain the bar's contribution to the conductivity and

---

[19] W. E. Lamb, Jr., *op. cit.*

[20] A. J. Bahr, "Theory of a Multimode Ring Laser with Internal Modulation," M. L. Report 1508, W. W. Hansen Laboratories of Physics, Stanford University, February 1967.

susceptibility tensors.

The circuit equations become self-consistent when the macroscopic polarization of the active medium is calculated from an assumed set of electric field amplitudes and phases.

The self-consistent equations are used to obtain information about the polarization and threshold population requirements of the OD traveling waves. We consider separately the effects the magnetic field and the birefringent bar have upon the threshold population. Their combined effect upon the threshold population is then considered. From these results an asymmetry in threshold population inversion is found to exist and its implications are discussed.

1.2. Circuit Equations

Assuming a spatial dependence of the electric field only on z where the $\hat{z}$ coordinate points along the direction of light propagation in the resonator and the $\hat{x}$ and $\hat{y}$ coordinates are orthogonal to $\hat{z}$, then Maxwell's equations can be written in mks units as

$$\nabla \times \underset{\sim}{E}(z,t) = -\frac{\partial \underset{\sim}{B}(z,t)}{\partial t} \qquad \nabla \cdot \underset{\sim}{D}(z,t) = 0$$

$$\nabla \times \underset{\sim}{H}(z,t) = \underset{\sim}{J}(z,t) + \frac{\partial \underset{\sim}{D}(z,t)}{\partial t} \qquad \nabla \cdot \underset{\sim}{B}(z,t) = 0 \qquad (1)$$

with

$$\underset{\sim}{D}(z,t) = \varepsilon_o \underset{\sim}{E}(z,t) + \underset{\sim}{P}(z,t) \qquad \underset{\sim}{B}(z,t) = \mu_o \underset{\sim}{H}(z,t) \tag{2}$$

where $\underset{\sim}{E}(z,t)$ is the total electric field in the cavity, and $\underset{\sim}{P}(z,t)$ is the polarization induced by the atomic medium. $\underset{\sim}{J}(z,t)$ is the current density. To provide for linear birefringence in the cavity, we use a second-rank susceptibility tensor $\underset{\approx}{\chi}$.[21] One can relate a cavity polarization $\underset{\sim}{P}(z,t)_{cav}$ to $\underset{\sim}{E}(z,t)$ through the tensor $\underset{\approx}{\chi}$ as[22]

$$\underset{\sim}{P}(z,t)_{cav} = \varepsilon_o \underset{\approx}{\chi}\, \underset{\sim}{E}(z,t) \tag{3}$$

Cavity losses can be introduced by using a current density to give

$$\underset{\sim}{J}(z,t)_{loss} = \underset{\approx}{\sigma}' \cdot \underset{\sim}{E}(z,t) \tag{4}$$

where $\underset{\approx}{\sigma}'$, which represents the phenomenological conductivity, is also a second-rank tensor. Since current density is equivalent to the time rate of change of polarization, we can combine Eqs. 3 and 4 to obtain[23]

$$\underset{\sim}{J}(z,t) = \underset{\approx}{\sigma} \cdot \underset{\sim}{E}(z,t) \tag{5}$$

where

$$\underset{\approx}{\sigma} = \underset{\approx}{\sigma}' + \varepsilon_o \underset{\approx}{\chi} \frac{\partial}{\partial t} \tag{6}$$

---

[21] M. Sargent, III, et al., *op. cit.*

[22] R. H. Pantell and H. E. Puthoff, *Fundamentals of Quantum Electronics*, John Wiley and Sons, Inc., 1969, p. 57.

[23] M. Sargent, III, et al., *op. cit.*

Substituting Eqs. 2 and 5 into Eq. 1 and eliminating $\underset{\sim}{H}(z,t)$, we obtain the wave equation

$$-\frac{\partial^2 \underset{\sim}{E}(z,t)}{\partial z^2} + \mu_o \underset{\approx}{\sigma} \cdot \frac{\partial}{\partial t} \underset{\sim}{E}(z,t) + \frac{1}{c^2} \frac{\partial^2 \underset{\sim}{E}(z,t)}{\partial t^2} = -\mu_o \frac{\partial^2 P(z,t)}{\partial t^2} \qquad (7)$$

The electromagnetic field can be expanded in terms of OD traveling wave modes, the modes being a combination of normal modes of the empty cavity having unknown amplitudes and phases.[24] This results in

$$\underset{\sim}{E}(z,t) = 2 \sum_{i=1}^{2} \sum_{n} \hat{e}_i \, E_{ni}^{+}(t) \sin\left(\Omega_{ni} t + \phi_{ni}^{+}(t) + \beta_{ni} z\right)$$

$$+ 2 \sum_{i=1}^{2} \sum_{n} \hat{e}_i \, E_{ni}^{-}(t) \sin\left(\Omega_{ni} t + \phi_{ni}^{-}(t) - \beta_{ni} z\right) \qquad (8)$$

where $E_{ni}^{\pm}(t)$ and $\phi_{ni}^{\pm}(t)$ are real slowly varying amplitude and phase quantities, the $\pm$ represent the two propagation directions, and the $\hat{e}_i$ are two orthogonal unit vectors, $\hat{x}$ and $\hat{y}$.

The empty cavity resonant frequencies $\left(\Omega_{ni}\right)$ are related to the wave numbers by

$$\Omega_{ni} = \beta_{ni} c \qquad (9)$$

---

[24] A. J. Bahr, *op. cit.*

where Ω_{nx} and Ω_{ny} correspond to waves having polarization perpendicular to the plane of the ring and in the plane of the ring, respectively. The wave numbers are given by $\beta_{nx}L = (2n + 1)\pi$ and $\beta_{ny}L = 2n\pi$, where L is the length of the cavity and n is a large integer on the order of 10^5. This difference in resonant frequencies is unique to a ring cavity having an odd number of cavity mirrors. For example, consider a wave emerging from point P in the cavity to be incident upon mirror No. 1 (see Fig. 1). If the wave has a polarization which is perpendicular to the plane of the ring, then at the mirror boundary this wave changes phase by approximately π, providing the angle of incidence is less than the Brewster angle of the material.[25] This phase change occurs at each of the three mirrors giving the wave a total additional phase change of 3π in traversing the cavity. However, a wave having a polarization in the plane of the ring sees no additional phase change in traversing the cavity. Thus, in the same physical length, the two waves see different optical path lengths, and hence the corresponding resonance conditions are different.

It is much easier to derive the circuit equations if Eq. 8 is rewritten in the form

$$\underset{\sim}{E}(z,t) = \sum_{i=1}^{2} \sum_{n} \hat{e}_i \left(A_{ni}(t) \sin \beta_{ni} z + \tilde{A}_{ni}(t) \cos \beta_{ni} z \right) \qquad (10)$$

where

---

[25] S. N. Bagaev, et al., *op. cit.*

$$A_{ni}(t) = E^{+}_{ni}(t)\, e^{-i\left(\Omega_{ni}t + \phi^{+}_{ni}(t)\right)} - E^{-}_{ni}(t)\, e^{-i\left(\Omega_{ni}t + \phi^{-}_{ni}(t)\right)} + c.c. \tag{11}$$

and

$$\tilde{A}_{ni}(t) = iE^{+}_{ni}(t)\, e^{-i\left(\Omega_{ni}t + \phi^{+}_{ni}(t)\right)} + iE^{-}_{ni}(t)\, e^{-i\left(\Omega_{ni}t + \phi^{-}_{ni}(t)\right)} + c.c. \tag{12}$$

Similarly the polarization may be written as[26]

$$\underset{\sim}{P}(z,t) = \sum_{i=1}^{2} \sum_{n} \hat{e}_i \left(P_{ni}(t) \sin \beta_{ni} z + \tilde{P}_{ni}(t) \cos \beta_{ni} z\right) \tag{13}$$

where the quantities $P_{ni}(t)$ and $\tilde{P}_{ni}(t)$ contain the amplitude and phase information regarding the polarization of the medium for the ni^{th} mode of the electric field. Thus, each of these quantities has, in general, two components for each propagation direction, one in phase with the ni^{th} mode of the electric field, and one in quadrature. Thus, we may write[27]

$$P_{ni}(t) = \left(C^{+}_{ni} + i\, S^{+}_{ni}\right) e^{-i\left(\Omega_{ni}t + \phi^{+}_{ni}\right)}$$

---

[26] A. J. Bahr, *op. cit.*

[27] *Ibid.*

$$+ \left(C_{ni}^{-} + i\, S_{ni}^{-}\right) e^{-i\left(\Omega_{ni} t + \phi_{ni}^{-}\right)} + \text{c.c.} \qquad (14)$$

and

$$\tilde{P}_{ni}(t) = \left(\tilde{C}_{ni}^{+} + i\, \tilde{S}_{ni}^{+}\right) e^{-i\left(\Omega_{ni} t + \phi_{ni}^{+}\right)}$$

$$+ \left(\tilde{C}_{ni}^{-} + i\, \tilde{S}_{ni}^{-}\right) e^{-i\left(\Omega_{ni} t + \phi_{ni}^{-}\right)} + \text{c.c.} \qquad (15)$$

As shown previously,[28] Eqs. 10 and 13 are substituted into Eq. 7 to obtain a set of circuit equations for the ni^{th} mode of the electric field. These equations are written as

$$\dot{E}_{ni}^{+} + \frac{1}{2\epsilon_o} \sum_{i=1}^{2} \left(\sigma_{ij}' \cos \psi_{nji}^{+} - \epsilon_o \Omega_{nj} \chi_{ij} \sin \chi_{nji}^{+}\right) E_{nj}^{+}$$

$$= -\frac{\nu}{4\epsilon_o} I_m \left\{\left(C_{ni}^{+} + \tilde{S}_{ni}^{+}\right) + i\left(S_{ni}^{+} - \tilde{C}_{ni}^{+}\right)\right.$$

$$\left. + \left[\left(C_{ni}^{-} + \tilde{S}_{ni}^{-}\right) + i\left(S_{ni}^{-} - \tilde{C}_{ni}^{-}\right)\right] e^{-i\Delta\phi_{ni}}\right\} \qquad (16)$$

---

[28] Technical Report MDL-Q31, Microwave Device and Physical Electronics Laboratory, University of Utah, Salt Lake City, Utah, December 1969.

$$\dot{\phi}^{+}_{ni} E^{+}_{ni} + \frac{1}{2\varepsilon_o} \sum_{j=1}^{2} \left(\sigma'_{ij} \sin \psi^{+}_{nji} + \varepsilon_o \Omega_{nj} \chi_{ij} \cos \psi^{+}_{nji} \right) E^{+}_{nj}$$

$$= - \frac{\nu}{4\varepsilon_o} R_e \left\{ \left(C^{+}_{ni} + \tilde{S}^{+}_{ni} \right) + i \left(S^{+}_{ni} - \tilde{C}^{+}_{ni} \right) \right.$$

$$\left. + \left[\left(C^{-}_{ni} + \tilde{S}^{-}_{ni} \right) + i \left(S^{-}_{ni} - \tilde{C}^{-}_{ni} \right) \right] e^{-i\Delta\phi_{ni}} \right\} \qquad (17)$$

$$\dot{E}^{-}_{ni} + \frac{1}{2\varepsilon_o} \sum_{i=1}^{2} \left(\sigma'_{ij} \cos \psi^{-}_{nji} - \varepsilon_o \Omega_{nj} \chi_{ij} \sin \psi^{-}_{nji} \right) E^{-}_{nj}$$

$$= - \frac{\nu}{4\varepsilon_o} I_m \left\{ \left(\tilde{S}^{-}_{ni} - C^{-}_{ni} \right) - i \left(\tilde{C}^{-}_{ni} + S^{-}_{ni} \right) \right.$$

$$\left. + \left[\left(\tilde{S}^{+}_{ni} - C^{+}_{ni} \right) - i \left(\tilde{C}^{+}_{ni} + S^{+}_{ni} \right) \right] e^{i\Delta\phi_{ni}} \right\} \qquad (18)$$

$$\dot{\phi}^{-}_{ni} E^{-}_{ni} + \frac{1}{2\varepsilon_o} \sum_{i=1}^{2} \left(\sigma'_{ij} \sin \psi^{-}_{nji} + \varepsilon_o \Omega_{nj} \chi_{ij} \cos \psi^{-}_{nji} \right) E^{-}_{nj}$$

$$= - \frac{\nu}{4\varepsilon_o} R_e \left\{ \left(\tilde{S}^{-}_{ni} - C^{-}_{ni} \right) - i \left(\tilde{C}^{-}_{ni} + S^{-}_{ni} \right) \right.$$

$$\left. + \left[\left(\tilde{S}^{+}_{ni} - C^{+}_{ni} \right) - i \left(\tilde{C}^{+}_{ni} + S^{+}_{ni} \right) \right] e^{i\Delta\phi_{ni}} \right\} \qquad (19)$$

where

$$\psi^{\pm}_{nji} = \left(\Omega_{nj} - \Omega_{ni}\right)t + \left(\phi^{\pm}_{nj} - \phi^{\pm}_{ni}\right) \tag{20}$$

$$\Delta\phi_{ni} = \phi^{-}_{ni} - \phi^{+}_{ni} \tag{21}$$

and ν is an average oscillating frequency.

By determining an expression for the polarization of the active medium in terms of amplitudes and phases of the OD waves, one can derive the S_{ni} and C_{ni} coefficients in terms of the electric field amplitudes using Eqs. 13 through 15. At this point the circuit equations become self-consistent in the amplitudes and phases of the electric field modes.

1.3. Polarization of the Medium

As discussed in the Lamb theory,[29] excited atoms in the medium are subjected to electric fields with assumed amplitudes and phases. The field frequencies are near the resonance of a pair of degenerate energy levels W_a and W_b. A magnetic field establishes a direction in space along which these energy levels are split due to the Zeeman broadening of the atom's energy state. The atoms interact with different frequencies not only because of Zeeman broadening but also

---

[29] W. E. Lamb, Jr., *op. cit.*

due to Doppler effects resulting from the thermal velocity distribution of the atoms.

The dipole moment exhibited by the atoms is driven by the electric field causing the atoms to become polarized. Using a density matrix formalism to describe an ensemble of such atoms, one can obtain an average dipole moment given by[30]

$$\underset{\sim}{P} = \text{trace } (\rho e\underset{\sim}{r}) \tag{22}$$

where $e\underset{\sim}{r}$ is the electric dipole moment operator, and ρ represents the density matrix.

A macroscopic polarization $\underset{\sim}{P}(z,t)$ is calculated from the average dipole moment by including contributions from all atoms in the medium which arrive at position z at time t regardless of the position z_o and time t_o at which they were excited. An expression for this polarization is given by Sargent,[31] et al., to be

$$\underset{\sim}{P}(z,t) = \sum_{\alpha} \int_{-\infty}^{t} dt_o \int dz_o \int dv\ \lambda_\alpha \left(z_o,t_o,v\right) \text{ trace}$$

$$\left[\rho\left(\alpha,z_o,t_o,v,t\right)e\underset{\sim}{r}\right]\ \delta\ \left[z - \left(z_o + v\left(t - t_o\right)\right)\right] \tag{23}$$

where v is the velocity of the atom, and $\lambda_\alpha\left(z_o,t_o,v\right)$ is assumed to

---

[30] R. H. Pantell and H. E. Puthoff, *op. cit.*, p. 31.

[31] M. Sargent, III, et al., *op. cit.*

be the number of atoms excited to state $\alpha = a,b$ per unit time per unit volume.

The differential equation of motion for the density matrix is given by[32]

$$\hbar\dot{\rho}\left(\alpha,z_o,t_o,v,t\right) = -i\ [H,\rho] - \frac{\hbar}{2}\ [\Gamma\rho + \rho\Gamma] \tag{24}$$

where Γ is the phenominological decay operator describing radiative decay of the atomic levels. It is assumed to be diagonal with elements γ_{m_α}. The hamiltonian H has the diagonal elements[33]

$$W_{m_\alpha} = W_\alpha + \mu_B g_\alpha H\ m_\alpha \tag{25}$$

where W_α is the zero magnetic field energy, H the magnetic field strength, μ_B the Bohr magneton, and g_α is the Lande g-factor. The off diagonals elements represent the time dependent perturbation energy and have the form

$$V_{m_a m_b}(t) = -\frac{1}{\hbar} \langle n_a J_a m_a \left| \underset{\sim}{E}(z,t) \cdot (e\underset{\sim}{r}) \right| n_b J_b m_b \rangle \tag{26}$$

where $\underset{\sim}{E}(z,t) = \underset{\sim}{E}\left[z_o + v\left(t - t_o\right),t\right]$ is the time dependent field "seen" by an excited atom at position $z = z_o + v\left(t - t_o\right)$ at time $t > t_o$. The eigenvectors $|n_\alpha J_\alpha m_\alpha\rangle$ are the basis vectors for the matrix representation of a system of atoms having a total angular momentum,

---

[32] *Ibid.*

[33] R. H. Pantell and H. E. Puthoff, *op. cit.*, p. 45.

z-component of angular momentum, and other quantum numbers represented, respectively, by J_α, m_α, and n_α.

Following the method of Sargent,[34] et al., we find that Eq. 26 can be reduced to

$$V_{m_a m_b}(t) = -\frac{P_{m_a m_b}}{\hbar}\left[\underset{\sim}{E}(z,t)\cdot(\hat{i}-i\hat{j})\,\delta_{m_a,m_b+1}\right.$$

$$\left.+\,\underset{\sim}{E}(z,t)\cdot(\hat{i}+i\hat{j})\,\delta_{m_a,m_b-1}\right] \qquad (27)$$

where $\hat{i}$ and $\hat{j}$ are unit vectors along the $\hat{x}$ and $\hat{y}$ directions, and the electric field $\underset{\sim}{E}(z,t)$ has been assumed to propagate in the $\hat{z}$ direction. The elements $P_{m_a m_b}$ can be written as[35]

$$P_{m_a m_b} = -\frac{p}{2}\left[\left(J_b \pm m_a\right)\left(J_b \pm m_a + 1\right)\right]^{1/2} \qquad m_a = m_b \mp 1 \qquad (28)$$

where the reduced matrix element p is equal to $\langle n_a J_a | er | n_b J_b \rangle$.

The electric field can now be substituted into Eq. 27 to determine the interaction hamiltonian. Substituting Eqs. 11 and 12 into Eq. 10, we obtain

$$\underset{\sim}{E}(z,t) = \frac{1}{2}\sum_i\sum_n \hat{e}_i\left\{\left[E^+_{ni}\, e^{i\left(\Omega_{ni}t+\phi^+_{ni}\right)} + E^+_{ni}\, e^{-i\left(\Omega_{ni}t+\phi^+_{ni}\right)}\right.\right.$$

---

[34] M. Sargent, III, et al., *op. cit.*

[35] E. U. Condon and G. H. Shortley, *The Theory of Atomic Spectra*, Cambridge University Press, New York, 1935, p. 63.

$$- E_{ni}^{-} e^{i\left(\Omega_{ni}t + \phi_{ni}^{-}\right)} - E_{ni}^{-} e^{-i\left(\Omega_{ni}t + \phi_{ni}^{-}\right)}\Big] \sin \beta_{ni} z$$

$$- i\Big[E_{ni}^{+} e^{i\left(\Omega_{ni}t + \phi_{ni}^{+}\right)} - E_{ni}^{+} e^{-i\left(\Omega_{ni}t + \phi_{ni}^{+}\right)}$$

$$+ E_{ni}^{-} e^{i\left(\Omega_{ni}t + \phi_{ni}^{-}\right)} - E_{ni}^{-} e^{-i\left(\Omega_{ni}t + \phi_{ni}^{-}\right)}\Big] \cos \beta_{ni} z\Big\} \qquad (29)$$

Then substituting Eq. 29 into Eq. 27 and defining $q = \pm 1$, we have

$$V_{m_a m_b}(t) = -\frac{P_{m_a m_b}}{2\hbar} \sum_i \sum_n \sum_q \delta_{m_a m_b + q} f_q(\hat{e}_i) \Big\{\sin \beta_{ni} \left[z_o + v\left(t - t_o\right)\right]$$

$$\Big[E_{ni}^{+} e^{i\left(\Omega_{ni}t + \phi_{ni}^{+}\right)} + E_{ni}^{+} e^{-i\left(\Omega_{ni}t + \phi_{ni}^{+}\right)}$$

$$- E_{ni}^{-} e^{i\left(\Omega_{ni}t + \phi_{ni}^{-}\right)} - E_{ni}^{-} e^{-i\left(\Omega_{ni}t + \phi_{ni}^{-}\right)}\Big]$$

$$- i \cos \beta_{ni} \left[z_o + v\left(t - t_o\right)\right]\Big[E_{ni}^{+} e^{i\left(\Omega_{ni}t + \phi_{ni}^{+}\right)}$$

$$- E_{ni}^{+} e^{-i\left(\Omega_{ni}t + \phi_{ni}^{+}\right)} + E_{ni}^{-} e^{i\left(\Omega_{ni}t + \phi_{ni}^{-}\right)}$$

$$- E_{ni}^{-} e^{-i\left(\hat{\Omega}_{ni} t + \phi_{ni}^{-}\right)}\Big]\Big\} \tag{30}$$

where

$$f_{\pm 1}\left(\hat{e}_i\right) = \hat{e}_i \cdot \left(\hat{i} \mp i\hat{j}\right) \tag{31}$$

The matrix elements of the hamiltonian given by Eqs. 25 and 30 can now be substituted into Eq. 24. As in Lamb,[36] a solution to the equation of motion is obtained using an iteration procedure. In this procedure we obtain contributions to the polarization in the first, third, etc., orders. Using only the first order solution, the polarization $\underset{\sim}{P}(z,t)$ is found, as shown previously,[37] to be

$$\underset{\sim}{P}(z,t) = -\frac{1}{2\kappa\beta u} \sum_j \sum_n \sum_q \sum_{m_a,m_b} f_q\left(\hat{e}_j\right)\left(\hat{i} + qi\hat{j}\right)\left|P_{m_a m_b}\right|^2 N_{m_a m_b}(z)$$

$$\cdot \Big[\left(\sin \beta_{nj} z + i \cos \beta_{nj} z\right) E_{nj}^{+} Z^{+} e^{-i\left(\Omega_{nj} t + \phi_{nj}^{+}\right)}$$

$$- \left(\sin \beta_{nj} z - i \cos \beta_{nj} z\right) E_{nj}^{-} Z^{-} e^{-i\left(\Omega_{nj} t + \phi_{nj}^{-}\right)}\Big] + \text{c.c.} \tag{32}$$

where βu is the Doppler line width. The terms $\left|P_{m_a m_b}\right|^2$ and $f_q\left(\hat{e}_j\right)$

---

[36] W. E. Lamb, Jr., *op. cit.*

[37] Technical Report MDL-Q34, Microwave Device and Physical Electronics Laboratory, University of Utah, Salt Lake City, Utah, October 1970.

are defined, respectively, in Eqs. 28 and 31. $Z^{\pm}$ is an abbreviated expression for $Z\left[i\left(\nu_{nj}^{\pm} - \omega_{m_a m_b}\right) - \gamma_{m_a m_b}\right]$ which is the plasma dispersion function discussed by Fried and Conte,[38] where $\hbar\omega_{m_\alpha m'_\alpha} = W_{m_\alpha} - W_{m'_\alpha}$, $\gamma_{m_\alpha m'_\alpha} = 1/2\left(\gamma_{m_\alpha} + \gamma_{m'_\alpha}\right)$, and $\nu_{nj}^{\pm}$ is the oscillating frequency of the $\pm$ propagation direction. The excitation density is defined as

$$N_{m_a m_b}(z) = \left[\frac{\Lambda_a(z)}{\gamma_{m_a m_a}} - \frac{\Lambda_b(z)}{\gamma_{m_b m_b}}\right] \tag{33}$$

where $\Lambda_\alpha(z)$ is the number of atoms excited to the state α per unit time per unit volume.

The excitation density $N_{m_a m_b}(z)$ for each direction is a constant with respect to z in the active medium, which we set equal to $N_{0m_a m_b}^{\pm}$. Outside the active medium the excitation density is zero.

Equation 32 is an expression for the macroscopic polarization in terms of the traveling wave amplitudes and phases of the nj^{th} electric field mode. As shown previously,[39] ni^{th} spatial Fourier components, $P_{ni}(t)$ and $\tilde{P}_{ni}(t)$, of the macroscopic polarization can be obtained by projecting $\underset{\sim}{P}(z,t)$ onto the respective normal modes $\hat{e}_i \sin \beta_{ni} z$ and $\hat{e}_i \cos \beta_{ni} z$. Then, by applying the definitions of Eqs. 14 and 15, the C_{ni} and S_{ni} coefficients are easily determined

---

[38] B. D. Fried and S. D. Conte, *The Plasma Dispersion Function (Hilbert Transform of the Gaussian)*, Academic Press, Inc., New York, 1961.

[39] Technical Report MDL-Q34, *op. cit.*

to be

$$C^{+}_{nx} = \tilde{S}^{+}_{nx} = -\bar{N}^{+}X^{+}_{1}E^{+}_{nx} + \bar{N}^{+}\left(X^{+}_{4}\cos\psi^{+}_{nyx} - X^{+}_{3}\sin\psi^{+}_{nyx}\right)E^{+}_{ny} \quad (34)$$

$$C^{-}_{nx} = -\tilde{S}^{-}_{nx} = \bar{N}^{-}X^{-}_{1}E^{-}_{nx} - \bar{N}^{-}\left(X^{-}_{4}\cos\psi^{-}_{nyx} - X^{-}_{3}\sin\psi^{-}_{nyx}\right)E^{-}_{ny} \quad (35)$$

$$S^{+}_{nx} = -\tilde{C}^{+}_{nx} = -\bar{N}^{+}X^{+}_{2}E^{+}_{nx} - \bar{N}^{+}\left(X^{+}_{3}\cos\psi^{+}_{nyx} + X^{+}_{4}\sin\psi^{+}_{nyx}\right)E^{+}_{ny} \quad (36)$$

$$S^{-}_{nx} = \tilde{C}^{-}_{nx} = \bar{N}^{-}X^{-}_{2}E^{-}_{nx} + \bar{N}^{-}\left(X^{-}_{3}\cos\psi^{-}_{nyx} + X^{-}_{4}\sin\psi^{-}_{nyx}\right)E^{-}_{ny} \quad (37)$$

$$C^{+}_{ny} = \tilde{S}^{+}_{ny} = -\bar{N}^{+}X^{+}_{1}E^{+}_{ny} - \bar{N}^{+}\left(X^{+}_{4}\cos\psi^{+}_{nyx} + X^{+}_{3}\sin\psi^{+}_{nyx}\right)E^{+}_{nx} \quad (38)$$

$$C^{-}_{ny} = -\tilde{S}^{-}_{ny} = \bar{N}^{-}X^{-}_{1}E^{-}_{ny} + \bar{N}^{-}\left(X^{-}_{4}\cos\psi^{-}_{nyx} + X^{-}_{3}\sin\psi^{-}_{nyx}\right)E^{-}_{nx} \quad (39)$$

$$S^{+}_{ny} = -\tilde{C}^{+}_{ny} = -\bar{N}^{+}X^{+}_{2}E^{+}_{ny} + \bar{N}^{+}\left(X^{+}_{3}\cos\psi^{+}_{nyx} - X^{+}_{4}\sin\psi^{+}_{nyx}\right)E^{+}_{nx} \quad (40)$$

$$S^{-}_{ny} = \tilde{C}^{-}_{ny} = \bar{N}^{-}X^{-}_{2}E^{-}_{ny} - \bar{N}^{-}\left(X^{-}_{3}\cos\psi^{-}_{nyx} - X^{-}_{4}\sin\psi^{-}_{nyx}\right)E^{-}_{nx} \quad (41)$$

where, in order to discuss threshold population requirements, we have defined

$$N^{\pm}_{o_{m_a m_b}} = \bar{N}^{\pm}\, D_{m_a m_b} \quad (42)$$

where $\bar{N}^{\pm}$ is a measure of the excitation density and $D_{m_a m_b}$ is a distribution function over the m_α sublevels and is independent of the excitation level,[40] and as shown previously[41] the X functions are found to be

$$X_1^{\pm} = \frac{\ell}{\hbar\beta u L} \sum_{m_a m_b} \left(\delta_{m_a,m_b-1} + \delta_{m_a,m_b+1}\right) |P_{m_a m_b}|^2 D_{m_a m_b} R_e\left(Z^{\pm}\right) \qquad (43)$$

$$X_2^{\pm} = \frac{\ell}{\hbar\beta u L} \sum_{m_a m_b} \left(\delta_{m_a,m_b-1} + \delta_{m_a,m_b+1}\right) |P_{m_a m_b}|^2 D_{m_a m_b} I_m\left(Z^{\pm}\right) \qquad (44)$$

$$X_3^{\pm} = \frac{\ell}{\hbar\beta u L} \sum_{m_a,m_b} \left(\delta_{m_a,m_b-1} - \delta_{m_a,m_b+1}\right) |P_{m_a m_b}|^2 D_{m_a m_b} R_e\left(Z^{\pm}\right) \qquad (45)$$

$$X_4^{\pm} = \frac{\ell}{\hbar\beta u L} \sum_{m_a,m_b} \left(\delta_{m_a,m_b-1} - \delta_{m_a,m_b+1}\right) |P_{m_a m_b}|^2 D_{m_a m_b} I_m\left(Z^{\pm}\right) \qquad (46)$$

where ℓ, L represent, respectively, the length of the active medium and the length of the cavity, and $R_e\left(Z^{\pm}\right)$, $I_m\left(Z^{\pm}\right)$ represent, respectively, the real and imaginary parts of the plasma dispersion function.

---

[40] M. Sargent, III, et al., *op. cit.*

[41] Technical Report MDL-Q34, *op. cit.*

1.4. Self-Consistent Equations

1.4.1. General Self-Consistent Equations

The self-consistent equations in terms of the traveling wave amplitudes and phases can now be derived by substituting Eqs. 34 through 41 into Eqs. 16 through 19. For the ni^{th} mode of the + direction, we obtain

$$\dot{E}^+_{nx} + \frac{\sigma'_{xx}}{2\varepsilon_o} E^+_{nx} + \frac{1}{2\varepsilon_o}\left(\sigma^{+\prime}_{xy} \cos \psi^+_{nyx} - \varepsilon_o \Omega_{ny} \chi^+_{xy} \sin \psi^+_{nyx}\right) E^+_{ny}$$

$$= \frac{\nu}{2\varepsilon_o} \bar{N}^+ X^+_2 E^+_{nx} + \frac{\nu}{2\varepsilon_o} \bar{N}^+ \left(X^+_3 \cos \psi^+_{nyx} + X^+_4 \sin \psi^+_{nyx}\right) E^+_{nx} \qquad (47)$$

$$\dot{E}^+_{ny} + \frac{\sigma'^+_{yy}}{2\varepsilon_o} E^+_{ny} + \frac{1}{2\varepsilon_o}\left(\sigma'^+_{yx} \cos \psi^+_{nyx} + \varepsilon_o \Omega_{nx} \chi^+_{yx} \sin \psi^+_{nyx}\right) E^+_{nx}$$

$$= \frac{\nu}{2\varepsilon_o} \bar{N}^+ X^+_2 E^+_{ny} - \frac{\nu}{2\varepsilon_o} \bar{N}^+ \left(X^+_3 \cos \psi^+_{nyx} - X^+_4 \sin \psi^+_{nyx}\right) E^+_{nx} \qquad (48)$$

$$\dot{\phi}^+_{nx} E^+_{nx} + \frac{\Omega_{nx} \chi^+_{xx}}{2} E^+_{nx} + \frac{1}{2\varepsilon_o}\left(\sigma'^+_{xy} \sin \psi^+_{nyx} + \varepsilon_o \Omega_{ny} \chi^+_{xy} \cos \psi^+_{nyx}\right) E^+_{ny}$$

$$= \frac{\nu}{2\varepsilon_o} \bar{N}^+ X^+_1 E^+_{nx} - \frac{\nu}{2\varepsilon_o} \bar{N}^+ \left(X^+_4 \cos \psi^+_{nyx} - X^+_3 \sin \psi^+_{nyx}\right) E^+_{ny} \qquad (49)$$

$$\dot{\phi}^+_{ny} E^+_{ny} + \frac{\Omega_{ny} \chi^+_{yy}}{2} E^+_{ny} + \frac{1}{2\varepsilon_o}\left(-\sigma'^+_{yx} \sin \psi^+_{nyx} + \varepsilon_o \Omega_{nx} \chi^+_{yx} \cos \psi^+_{nyx}\right) E^+_{nx}$$

$$= \frac{\nu}{2\varepsilon_o} \bar{N}^+ X_1^+ E_{ny}^+ + \frac{\nu}{2\varepsilon_o} \bar{N}^+ \left(X_4^+ \cos \psi_{nyx}^+ + X_3^+ \sin \psi_{nyx}^+ \right) E_{nx}^+ \qquad (50)$$

The analogous equations for the nith mode of the OD wave are obtained by replacing the "+" superscript with a "-" superscript. Thus we see that for each propagation direction, four coupled equations describe the nth mode of the electric field. The equations involving $\dot{E}_{ni}^{\pm}$ are referred to as the amplitude equations, and those involving $\dot{\phi}_{ni}^{\pm}$ are referred to as the reactive balance equations. By using computer techniques these equations are solvable for each mode, yielding simultaneously the polarization, phase, and threshold population inversion. We will not carry out such a detailed solution of these first order equations since it cannot provide significantly more meaningful results than a qualitative analysis of the equations provides.

1.4.2. Amplitude Equations

For the purpose of discussion we consider only the equation involving $\dot{E}_{nx}^+$ (Eq. 47) since similar statements hold for the $\dot{E}_{ny}^+$ equation and for modes of the - direction. Under the condition of steady state, $\dot{E}_{nx} = 0$ and Eq. 47 reduces to four groups of terms. The two groups on the left-hand side concern the cavity parameters of loss and birefringence. The two groups on the right-hand side concern the action of the active medium.

The first group on the left-hand side containing the term

$\sigma'_{xx}/2\varepsilon_o$ is the average loss encountered by the $\hat{x}$ component of the n^{th} + propagation mode. The second group on the left-hand side represents the coupling of E^+_{ny} to E^+_{nx} resulting from loss anisotropy and linear birefringence represented, respectively, by σ'^+_{xy} and χ^+_{xy}. Thus, if parameters σ'^+_{xy} and χ^+_{xy} go to zero, there would be no coupling between the components from the cavity parameters.

The first group on the right-hand side contains the term $\nu\bar{N}^+X_2^+/2\varepsilon_o$, which represents the unsaturated gain encountered by the E^+_{nx} field component, where $\bar{N}^+$ is the population inversion density for the + propagation direction. The second group on the right-hand side, containing the X_3^+ and X_4^+ functions, describe the coupling effects of the active medium. As shown previously,[42] the X functions can be rewritten approximately as

$$X_1^+ \simeq -\frac{10\ell p^2 D_1}{\hbar\beta u L}\left[\left(\frac{\nu^+_{ni}-\omega_{12}+\gamma H}{\beta u}\right)e^{-\left(\frac{\nu^+_{ni}-\omega_{12}-\gamma H}{\beta u}\right)^2}\right.$$

$$\left.+\left(\frac{\nu^+_{ni}-\omega_{12}-\gamma H}{\beta u}\right)e^{-\left(\frac{\nu^+_{ni}-\omega_{12}-\gamma H}{\beta u}\right)^2}\right] \qquad (51)$$

$$X_2^+ \simeq \frac{5\pi^{1/2}\ell p^2 D_1}{\hbar\beta u L}\left[e^{-\left(\frac{\nu^+_{ni}-\omega_{12}+\gamma H}{\beta u}\right)^2}+e^{-\left(\frac{\nu^+_{ni}-\omega_{12}-\gamma H}{\beta u}\right)^2}\right] \qquad (52)$$

---

[42] *Ibid.*

$$X_3^+ \simeq -\frac{10\ell p^2 D_2}{\hbar\beta u L}\left[\left(\frac{\nu_{ni}^+ - \omega_{12} + \gamma H}{\beta u}\right) e^{-\left(\frac{\nu_{ni}^+ - \omega_{12} + \gamma H}{\beta u}\right)^2}\right.$$

$$\left. - \left(\frac{\nu_{ni}^+ - \omega_{12} - \gamma H}{\beta u}\right) e^{-\left(\frac{\nu_{ni}^+ - \omega_{12} - \gamma H}{\beta u}\right)^2}\right] \tag{53}$$

$$X_4^+ \simeq \frac{5\pi^{1/2}\ell p^2 D_2}{\hbar\beta u L}\left[e^{-\left(\frac{\nu_{ni}^+ - \omega_{12} + \gamma H}{\beta u}\right)^2} - e^{-\left(\frac{\nu_{ni}^+ - \omega_{12} - \gamma H}{\beta u}\right)^2}\right] \tag{54}$$

where

$$D_1 = \sum_{m_a m_b} \left(\delta_{m_a, m_b - 1} + \delta_{m_a, m_b + 1}\right) D_{m_a m_b} \tag{55}$$

$$D_2 = \sum_{m_a m_b} \left(\delta_{m_a, m_b - 1} - \delta_{m_a, m_b + 1}\right) D_{m_a m_b} \tag{56}$$

The term $\gamma = \mu_B g/\hbar$ and H is the magnetic field strength. The oscillating frequency is ν_{ni}^+, and ω_{12} is the degenerate transition frequency between states a and b.

We assume there are three separate homogeneous regions in the active medium. One region is that portion of the active medium between the electromagnets, the other two being the portions of the active medium where each electromagnet is placed (see Fig. 1). The contributions of these regions are added together to give the X functions. For reasons explained in chapter II, the two electromagnets were operated with their fields opposing each other. If the magnetic fields are balanced, then the X_3^+ and X_4^+ terms are readily

found to be zero, and there is no coupling between the E^+_{nx} and E^+_{ny} field components. As a differential magnetic field is applied by unbalancing the current to the electromagnets, the X^+_3 and X^+_4 terms become nonzero and couple the field components. The principal gain term X^+_2 is nonzero for all magnetic field values, and is typically much larger than the coupling terms X^+_3 and X^+_4.

It is important to note from Eqs. 51 through 54 that all X functions have approximately the same value for the + and - waves. Consequently, the magnetic field effects on the two OD waves are essentially the same. One also notes from Eqs. 47 through 50 that there is no coupling between the OD waves in first order.

1.4.3. Reactive Balance Conditions

Equations 49 and 50 are referred to as the reactive balance equations. Using Eqs. 47 and 48 in Eqs. 49 and 50, we can obtain solutions for the quantities ϕ_{nx} and ϕ_{ny} which contain information about the oscillating frequencies. The oscillating frequencies ν_{nx} and ν_{ny} are related to $\dot{\phi}_{nx}$ and $\dot{\phi}_{ny}$ in the following way:

$$\nu_{nx} = \Omega_{nx} + \dot{\phi}_{nx}$$

$$\nu_{ny} = \Omega_{ny} + \dot{\phi}_{ny} \qquad (57)$$

where Ω_{nx} and Ω_{ny} are the empty cavity eigenfrequencies defined in Eq. 9.

Considering Eq. 49 we see that the nx + mode experiences a

frequency shift resulting from linear birefringence represented by the term $\Omega_{nx}\chi^{+}_{xx}/2$. Additional frequency effects occur in the form of cavity coupling terms when σ'_{xy} and/or χ_{xy} are nonzero. Frequency pulling due to the presence of the active medium results from the term $\nu\bar{N}^{+}X^{+}_{1}/2\varepsilon_{o}$. Additional coupling effects also result from the magnetic field and are represented by the last group on the right-hand side of Eq. 49.

The eigenfrequencies Ω_{nx} and Ω_{ny} correspond to waves having polarization perpendicular to the plane of the ring and in the plane of the ring, respectively. As we have shown previously, the eigenfrequencies Ω_{nx} are displaced from the eigenfrequencies Ω_{ny} by $\Delta\Omega = \pi c/L$. In order to support oscillation of waves with an electric field vector having a component not only perpendicular to the plane of the ring, but also in the plane of the ring, we require that components along each direction have the same oscillating frequency, i.e., $\nu_{nx} = \nu_{ny}$. For this to hold we must have, from Eq. 57,

$$\dot{\phi}_{nx} = \dot{\phi}_{ny} + (2k + 1)\frac{\pi c}{L} \qquad k = 0,1,2, \qquad (58)$$

The index k is allowed to take on values other than zero. This accounts for cavity birefringence, etc., which causes a different refractive index to be "seen" by waves having their field components directed along the $\hat{x}$ direction as opposed to directed along the $\hat{y}$ direction. Using this condition in Eq. 49 and subtracting the result from Eq. 50, we obtain

$$\frac{E^+_{nx}}{E^+_{ny}}\left[\frac{\nu\bar{N}^+}{2\varepsilon_o}\left(X^+_4\cos\psi^+_{nyx}+X^+_3\sin\psi^+_{nyx}\right)+\frac{1}{2\varepsilon_o}\left(-\sigma^+_{yx}\sin\psi^+_{nyx}\right.\right.$$

$$\left.+\varepsilon_o\Omega_{nx}\chi^+_{yx}\cos\psi^+_{nyx}\right)\Bigg]+\frac{E^+_{ny}}{E^+_{nx}}\left[\frac{\nu\bar{N}^+}{2\varepsilon_o}\left(X^+_4\cos\psi^+_{nyx}-X^+_3\sin\psi^+_{nyx}\right)\right.$$

$$\left.-\frac{1}{2\varepsilon_o}\left(\sigma'^+_{xy}\sin\psi^+_{nyx}+\varepsilon_o\Omega_{ny}\chi^+_{xy}\cos\psi^+_{nyx}\right)\right]$$

$$=(2k+1)\frac{c}{2L}-\frac{1}{2}\left(\Omega_{ny}\chi^+_{yy}-\Omega_{nx}\chi^+_{xx}\right) \tag{59}$$

The similar result for the OD wave is obtained by replacing the "+" superscripts by "−" superscripts. The only waves which can be resonant in the cavity are those which satisfy Eq. 59. These waves will in general have an elliptical polarization with electric field components along $\hat{x}$ and $\hat{y}$, differing in phase by ψ_{nyx} while having an amplitude ratio E_{nx}/E_{ny}. As the bar is varied in angular position, the σ' and χ terms will change. Likewise, as the magnetic field in the active medium region is varied, the X terms change. These variations cause the parameters in the reactive balance equation (Eq. 59) to vary. Hence, waves satisfying the new conditions will have a different phase and/or amplitude ratio from the waves satisfying the previous condition. Thus, we can say that as the bar is varied in angular position and/or the magnetic field is changed, the resonant waves will in general experience a change in polarization.

One can also predict that, if the combined parameter variations are different for the two directions, the polarization of the OD waves will change differently. As discussed above and shown previously,[43] the X functions have approximately the same values for the + and - directions. We must therefore determine how the σ' and χ terms vary as a function of bar orientation, and whether they are different for the two propagation directions.

1.4.4. The σ' and χ Terms

To calculate the σ' and χ matrix elements, we begin by deriving a transfer function which describes light propagation from the active medium through the birefringent bar. From a given point in the active medium, the bar appears different for the two propagation directions since in one direction waves from the active medium region reflect from one cavity mirror before entering the bar, and for the opposite direction waves reflect from two cavity mirrors before entering the bar. Thus, two transfer functions are necessary, one describing each propagation direction.

For waves reflecting from one cavity mirror before entering the bar, the $\hat{x}$ component suffers an additional π phase shift from the $\hat{y}$ component, thus the components will have optical path lengths differing by $\lambda/2$ from any given point in the medium to the entrance point on the surface of the bar. We can account for this in the transfer function by replacing $\underset{\sim}{E}_x$ by $\underset{\sim}{E}_x e^{i\pi} = -\underset{\sim}{E}_x$, and then

---

[43] *Ibid.*

transforming to the bar coordinate system which is at some angular orientation with respect to the laser coordinate system. For the opposite direction waves reflect from two cavity mirrors before entering the bar. Therefore, the path lengths of the $\hat{x}$ and $\hat{y}$ components differ by λ from a given point in the medium to the entrance point on the bar's surface, and hence there is no coordinate reversal. Thus, we may transform the $\hat{x}$ and $\hat{y}$ field components directly to the bar coordinate system.

In order to relate the σ' and χ terms to the transfer functions, each function is separated into a fictitious loss and birefringent element. The combination of the two elements is required to have the same transmission characteristics as the transfer function.[44] From the loss element a phenomenological σ' tensor is found having an equivalent loss distributed evenly over the cavity. Similarly the birefringent element is used to determine the phenomenological χ tensor having an equivalent birefringence distributed evenly over the cavity.

As localized elements occupying a small region of the cavity, the bar and Brewster windows cannot be treated as a perturbation on the existing normal modes. Thus, we distributed their effects over the cavity such that they could be treated as perturbation terms.[45,46]

---

[44] G. N. Ramachandran and S. Ramasheshan, "Crystal Optics," *Handbuch der Physik*, Vol. XXV/1, Sections 12 and 13.

[45] W. E. Lamb, Jr., *op. cit.*

[46] M. Sargent, III, et al., *op. cit.*

As shown previously,[47] these operations result in the following matrix elements:

$$\sigma_{yy}'^{+} \simeq 7 \times 10^{-4} \qquad \sigma_{yy}'^{-} \simeq 7 \times 10^{-4}$$

$$\sigma_{xx}'^{+} \simeq .67 \times 10^{-4} \qquad \sigma_{xx}'^{-} \simeq .67 \times 10^{-4}$$

$$\sigma_{xy}'^{+} = \sigma_{yx}'^{+} \simeq -.041\alpha \times 10^{-4} \qquad \sigma_{xy}'^{-} = \sigma_{yx}'^{-} = .041\alpha \times 10^{-4}$$

$$\varepsilon_o \nu \chi_{xy}'^{+} = \varepsilon_o \nu \chi_{yx}'^{+} \simeq .74\alpha \times 10^{-4} \qquad \varepsilon_o \nu \chi_{xy}'^{-} = \varepsilon_o \nu \chi_{yx}'^{-} \simeq = -.74\alpha \times 10^{-4} \tag{60}$$

where α is bar rotation about the transverse axis in degrees (see Fig. 3 and discussion in chapter II). The effects of Brewster window loss have been included in the σ_{yy}' and σ_{xx}' terms.

One notes from Eq. 60 that the coupling terms (off diagonal matrix elements) are opposite in sign for the two propagation directions.

1.5 Discussion

We conclude that for a given set of parameter values in Eq. 59, there is a particular value of E_{nx}^{+}/E_{ny}^{+} and ψ_{nyx}^{+} which will satisfy the equation. When these parameters are changed, the polarization, that is,

---

[47] Technical Report MDL-Q33, Microwave Device and Physical Electronics Laboratory, University of Utah, Salt Lake City, Utah, July 1970.

E^+_{nx}/E^+_{ny} and ψ^+_{nyx} will vary. One notes from Eq. 60 that the coupling terms (off diagonal matrix elements) are opposite in sign for the two propagation directions. Thus the parameters in the reactive balance equation change differently for the + and - directions leading to different polarization changes between the OD waves.

If we had modeled a four-mirror cavity instead of the three-mirror cavity, each wave would have suffered the same additional phase shift in going from the active medium to the bar. Consequently, the σ' and χ terms for the two directions would be the same. In this case, we would not expect different changes in the polarization of the OD waves for small rotations of the bar.

We would like to make predictions about the amplitudes of the OD waves as a function of differential magnetic field and bar orientation. Indications about the relative amplitudes can be obtained from the threshold population $\left(\bar{N}_{Th}\right)$, the threshold population being the minimum inversion necessary to overcome the cavity losses. We argue that waves having a threshold population requirement which is higher than other waves will tend to have a lower oscillating amplitude. To obtain the threshold population Eq. 47 is substituted into Eq. 48 and the result is solved for $\bar{N}$. Upon doing this for the + wave, we obtain an approximate expression for $\bar{N}^+_{Th}$; the corresponding expression for the - wave is obtained by replacing the + superscripts with - superscripts.

$$\bar{N}^{\pm}_{Th} \simeq \frac{\sigma'^{\pm}_{xx}}{\nu X^{\pm}_2}\left(1 - \frac{\sigma'^{\pm}_{xx}}{4\sigma'^{\pm}_{yy}}\right) + \frac{1}{\sigma'^{\pm}_{yy}\nu X^{\pm}_2}\left[\left(\varepsilon_o \nu \chi^{\pm}_{xy}\right)^2 \sin^2 \psi^{\pm}_{nyx} - \sigma'^{\pm 2}_{xy} \cos^2 \psi^{\pm}_{nyx}\right]$$

$$+\frac{1}{\left(\nu X_2^{\pm}\right)^3}\left[\left(\nu X_3^{\pm}\right)^2\cos^2\psi_{nyx}^{\pm}-\left(\nu X_4^{\pm}\right)^2\sin^2\psi_{nyx}^{\pm}\right]$$

$$+\frac{\sigma_{xx}^{'\pm}\left[\nu X_3^{\pm}\,\varepsilon_o\nu\chi_{xy}^{\pm}+\nu X_4^{\pm}\,\sigma_{xy}^{'\pm}\right]\sin 2\psi_{nyx}^{\pm}}{2\sigma_{yy}^{'\pm}\left(\nu X_2^{\pm}\right)^2}+\text{smaller terms} \qquad (61)$$

where we have assumed $\sigma_{yy}^{'\pm} >> \sigma_{xx}^{'\pm}$, $\sigma_{xy}^{'\pm}$, $\varepsilon_o\nu\chi_{xy}^{\pm}$ and $X_2^{\pm} >> X_3^{\pm}, X_4^{\pm}$. The σ' and χ terms are given in Eq. 60, while the X terms are given in Eqs. 52 through 54.

Equation 61 is valid providing E_{nx} and E_{ny} are not zero. For example, if the opposing magnetic fields are balanced and the bar is oriented with $\alpha = 0$, then the terms X_3^{+}, X_4^{+}, $\sigma_{xy}^{'+}$ and $\chi_{xy}^{'+}$ are zero, and no coupling takes place between the field components. The field component E_{ny}, which has high loss, consequently is below threshold and therefore is zero. Thus, we must derive the expression for threshold population from Eq. 47.

Upon doing this we obtain the expression

$$\bar{N}_{Th}^{\pm} = \frac{\sigma_{xx}^{'\pm}}{\nu X_2^{\pm}} \qquad (62)$$

We see from this equation the minimum condition for oscillation is determined by the loss along the $\hat{x}$ direction. The $\nu X_2^{\pm}$ term is associated with the unsaturated gain each mode receives in passing through the active medium.

Consider the case where the bar is in the null position, i.e., σ'_{xy} and χ_{xy} are zero. Under these conditions a differential field is set up by unbalancing the current to the electromagnets causing $X_3^{\pm}$ and $X_4^{\pm}$ to become nonzero. Now both E_{nx} and E_{ny} are nonzero, because of the coupling terms, and we can use Eq. 61 to obtain an expression for the corresponding threshold population. Upon doing this we obtain

$$\bar{N}_{Th}^{\pm} \simeq \frac{\sigma'_{xx}}{\nu X_2^{\pm}} \left(1 - \frac{\sigma'^{\pm}_{xx}}{4\sigma'^{\pm}_{yy}} \right) + \frac{\left(\nu X_3^{\pm}\right)^2 \cos^2 \psi_{nyx}^{\pm} - \left(\nu X_4^{\pm}\right)^2 \sin^2 \psi_{nyx}^{\pm}}{\left(\nu X_2^{\pm}\right)^2} \tag{63}$$

We note from this equation that $N_{Th}^{\pm}$ increases as the differential field is applied provided

$$\left(\nu X_3^{\pm}\right)^2 \cos^2 \psi_{nyx}^{\pm} > \left(\nu X_4^{\pm}\right)^2 \sin^2 \psi_{nyx}^{\pm} \tag{64}$$

We find that for most of the oscillating modes, i.e., twelve of the twelve to fifteen oscillating modes, $|\nu X_3^{\pm}| > |\nu X_4^{\pm}|$. The only modes which do not obey this inequality are those located furthest from line center, and these modes have small amplitudes if they oscillate at all. If the phase angle $\psi_{nyx}^{\pm}$ is near 90°, the inequality in Eq. 64 would not hold. However, experimentally we find that $\psi_{nyx}^{\pm}$ is a relatively small angle for both directions. But this experiment was performed in the oscillating laser which would give some weighted average ψ over all oscillating modes. If we assume, though, that ψ_{nyx}

does not vary appreciably from mode to mode, Eq. 64 is easily satisfied for the oscillating modes, and the threshold population will increase for all modes in either direction as the differential magnetic field is applied to the active medium. Consequently, we are lead to believe that in the oscillating laser, the amplitudes of the OD waves will decrease as the differential field is applied.

Consider now the case of rotating the bar such that σ'_{xy} and χ_{xy} are nonzero while maintaining balanced magnetic fields. In this situation Eq. 61 can be written as

$$\bar{N}^{\pm}_{Th} = \frac{\sigma'^{\pm}_{xx}}{\nu X^{\pm}_2}\left(1 - \frac{\sigma'^{\pm}_{xx}}{4\sigma'^{\pm}_{yy}}\right) + \frac{1}{\sigma'^{\pm}_{yy}\nu X^{\pm}_2}\left[\left(\varepsilon_o \nu \chi^{\pm}_{xy}\right)^2 \sin^2 \psi^{\pm}_{nyx} - \sigma'^{\pm 2}_{xy} \cos^2 \psi^{\pm}_{nyx}\right] \tag{65}$$

We note from Eq. 60 that $|\varepsilon_o \nu \chi_{xy}| >> |\sigma'_{xy}|$ and the second factor of Eq. 65 is positive provided $\psi^{\pm}_{nyx}$ is greater than approximately 3° which we find, experimentally, to be true for the average ψ_{nyx} mentioned above. Thus, as α is increased by rotating the bar, the threshold population requirement increases for both directions since $(\chi_{xy})^2$ is positive. This indicates that the oscillating amplitude for modes in both directions will decrease as the bar is rotated away from $\alpha = 0$.

As a final case we consider the combined differential magnetic field and birefringent bar at $\alpha \neq 0$. Now all terms of Eq. 61 are nonzero and, as discussed, the second and third terms are positive, adding to the first term. However, the fourth term behaves differently. It

can be written approximately as

$$+\frac{\sigma'_{xx}\left(\nu X_3^{\pm}\right)\left(\varepsilon_o \nu\chi_{xy}^{\pm}\right)\sin 2\psi_{nyx}^{\pm}}{2\sigma'^{\pm}_{yy}\left(\nu X_2^{\pm}\right)^2} \tag{66}$$

where we have assumed $\varepsilon_o \nu\chi_{xy}^{\pm} >> \sigma'^{\pm}_{xy}$ as shown in Eq. 60. As discussed above and as shown previously,[48] the term $\nu X_3^{\pm}$ for each mode is essentially independent of the propagation direction. The angle $2\psi_{nyx}^{\pm}$ has been found experimentally to be between 0 and 90 degrees for both + and - propagation directions. However, as discussed above, this is an average ψ over all oscillating modes. The term $\varepsilon_o \nu\chi_{xy}$ changes sign with propagation direction. As a consequence Eq. 66 adds to the first three terms of Eq. 61 causing an increase in $\bar{N}_{Th}$, but for the opposite direction it subtracts from these terms causing a drop in $\bar{N}_{Th}$ relative to the opposite direction. If the bar is rotated in the opposite direction ($-\alpha$), the opposite will occur, i.e., $\bar{N}_{Th}$ for the direction which increased for $+\alpha$ will now decrease while the OD wave will experience as increase in $\bar{N}_{Th}$. We can therefore predict an asymmetry in the threshold population of the OD waves, the asymmetry being caused by the combination of a differential magnetic field and a birefringent bar placed in a three-mirror ring cavity. This implies that an amplitude asymmetry is likely to occur in the oscillating laser. If we had used a four-mirror ring cavity, the asymmetry in $\bar{N}_{Th}$

---

[48] Technical Report MDL-Q34, *op. cit.*

would not exist since the χ_{xy} and σ'_{xy} terms would not change sign for the two propagation directions and we would not expect an amplitude asymmetry to occur.

II. EXPERIMENTAL RESULTS

2.1. Introduction

Asymmetric amplitude changes can be induced between the OD traveling waves in a three-mirror ring laser cavity. These changes are found to occur for certain orientations of an inner-cavity birefringent bar when an axial magnetic field is applied to the active medium.

We describe experimentally the behavior of the amplitude changes in a laser operating in twelve to fifteen free-running modes. The amplitude asymmetries are shown to be accompanied by asymmetric polarization changes. Asymmetric polarization changes are also found to exist on a single pass when two elements are utilized, one of which causes reciprocal changes to occur in the polarization of the OD waves, the other of which causes nonreciprocal changes to occur in the OD wave's polarization. We show that an element causing such nonreciprocal changes is the active medium in the presence of an axial magnetic field, and how a birefringent bar placed in a three-mirror cavity can be made to induce reciprocal changes in the polarization of OD waves. We describe how the theory predicts that this combination of elements also leads to the observed amplitude asymmetries. Additional supporting experiments which give greater insight into the operation of the device are presented; however, an explanation of these results in terms of the theory is not attempted.

2.2. Experimental Apparatus

The ring cavity is mounted on a 5' x 6' slab as shown in Fig. 2. The three-legged cavity has a total length of 410 cm. Each mirror is the dielectric layer type with a transmission of 0.05 percent. The amplifier tube is placed in one leg of the cavity, and has an active length of 125 cm. The laser operates at λ = 6328 Å. The plasma is dc excited and is sustained between a centrally located cathode and two anodes which are near each end of the tube. The current in each leg is approximately 35 mA. The ID of the bore is 3 mm, which restricts operation to the fundamental transverse mode. Brewster-angle windows of fused silica glass enclose the ends of the tube; they are aligned with each other to ±5 minutes. The tube is filled to a total pressure of approximately 1.3 torr. A mixture of 5.5 to 1, He^3 to Ne^{20} (99.95 percent isotopically pure), was used. With this pressure and mixture, the tube has a single-pass gain of approximately 10 percent. In most of the experiments which are described, the laser operated in twelve to fifteen free-running modes.

Two electromagnets, each 34 cm in length, are symmetrically placed over the amplifier tube as shown in Fig. 2. Each magnet supplies an axial magnetic field of approximately 67 gauss/amp.

The inner-cavity birefringent bar is a 6 x 2 x 20 mm quartz crystal. The c-axis is along the long length of the bar; the other axes lie in the 2 and 6 mm directions. The bar is housed in a gimbal mount which allows rotations about three axes which intersect in the middle of the bar. The "longitudinal" axis lies in the intersection

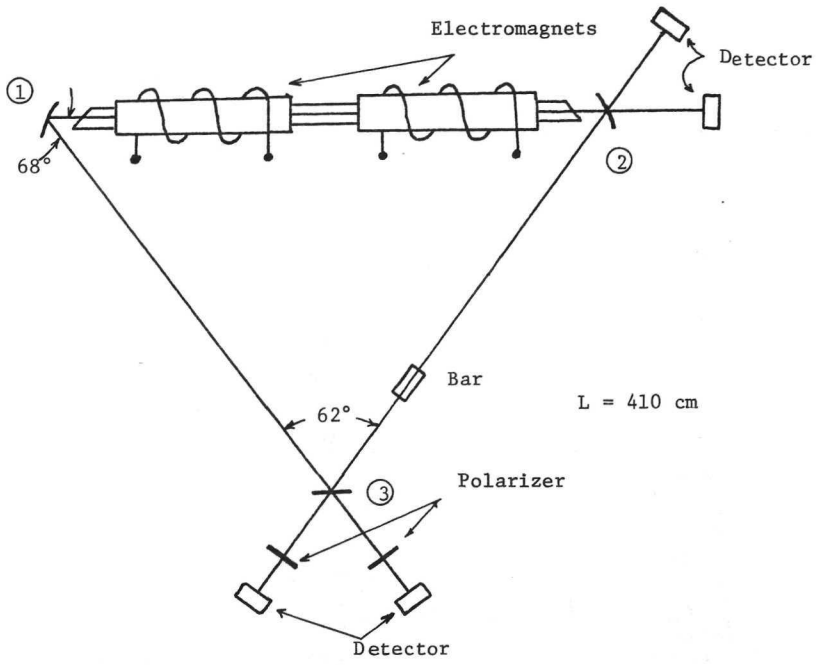

(a)

(b)

Fig. 2a. Schematic diagram of the ring laser showing the position of the electromagnets and the quartz bar. The polarization of the OD waves is measured from the output of mirror No. 3, while their amplitudes are measured from the output of mirror No. 2. R = 6 m, 3 m, and infinity for mirrors Nos. 1, 2 and 3, respectively.

b. Picture of the ring laser.

of the plane of the ring and the plane normal to the beam in which the bar is placed. The "transverse" axis is perpendicular to the longitudinal axis and makes an angle θ with the plane of the ring (see Fig. 3). The angle θ is varied by rotating the transverse axis about the longitudinal axis. The "normal" axis is perpendicular to the entrance and exit surfaces of the quartz bar, and moves with the bar as shown in Fig. 3. The bar's c-axis is aligned along the transverse axis.

2.3. Bidirectional Operation

Bidirectional operation, i.e., simultaneous oscillation of waves traveling in both the clockwise (cw) and counterclockwise (ccw) directions, is necessary for successful orientation sensing. In large multimode ring lasers utilizing a single neon isotope, unidirectional operation predominates.[49] However, we find that when a current of approximately 2 amps is supplied to each electromagnet, stable bidirectional operation occurs. These unidirectional effects result from gain competition between the oppositely directed (OD) waves, which is presumably the multimode analogy to the single mode competition effects discussed by Aronowitz.[50] In the single-mode case, the competition is reduced by using a mixture of Ne^{20} and Ne^{22},

---

[49] R. Pohle, "A Possible Explanation of Unidirectionality of Large Ne^{20} Ring Lasers," Physics Department, University of Maryland, College Park, Maryland, unpublished, June 6, 1967.

[50] F. Aronowitz, *op. cit.*

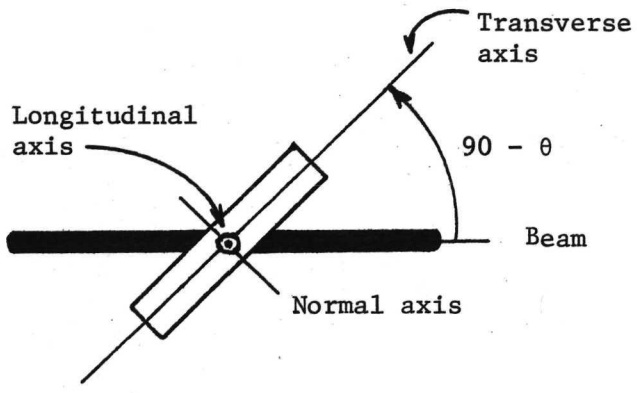

(a)

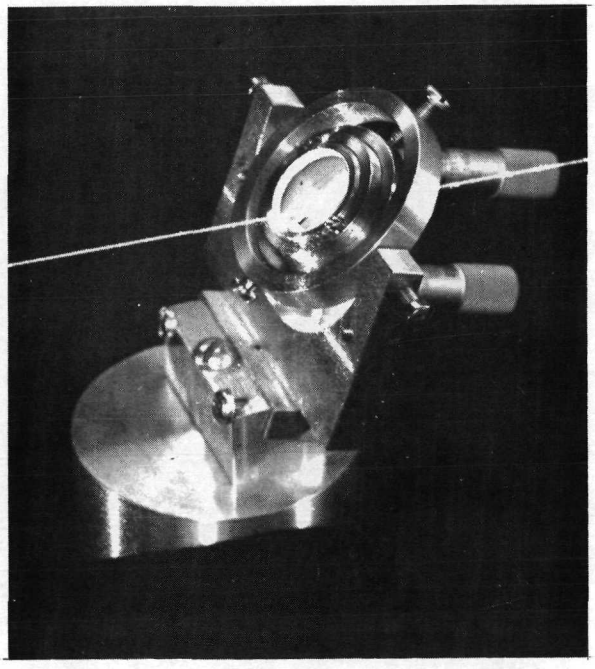

(b)

Fig. 3a. Schematic diagram of the quartz bar showing the three axes; the bar's c-axis is aligned along the transverse axis.

b. Enlarged view of the bar.

which produces two Doppler gain profiles separated by the isotopic shift. It is probable that in our case the competition is reduced in a similar way by producing two Doppler profiles separated by twice the Zeeman shift. While allowing bidirectional operation, the magnetic field also quenches any oscillation at $\lambda = 3.39\ \mu$ which may be present.[51]

2.4. Asymmetric Amplitude and Polarization Changes

As indicated in Fig. 3 the bar is placed in the ring cavity with its c-axis along the transverse axis. Balanced opposing magnetic fields are applied to the active medium by supplying a current of 3 amps to each electromagnet. This maintains bidirectional operation while presumably canceling any induced polarization rotating effects caused by the fields. Under these conditions the average power in each direction is "normalized" to the same value. Upon producing a differential axial field of 167 gauss (decreasing the current in one magnet to 1.75 amps and increasing the other to 4.25 amps), we find that at certain bar orientations, the average power in one direction increases while the average power in the other direction decreases, or, equivalently, there is an amplitude asymmetry in the OD waves.

The asymmetric effect has the following characteristics. If $\alpha = 0$, that is, if the normal axis is initially positioned in the "null plane," i.e., the plane formed by the beam and transverse axis,

---

[51] W. E. Bell, A. L. Bloom, "Zeeman Effect at 3.39 Microns in a Helium-Neon Laser," *Applied Optics*, Vol. 3, No. 3, March 1964, pp. 413-415.

the amplitude of the OD waves remains essentially constant as the differential magnetic field is applied to the active medium. However, if the bar is rotated so that the normal axis rotates about the transverse axis out of the null plane, ($\alpha \neq 0$), then, upon applying the same field, the amplitude of one wave increases while the amplitude of the OD wave decreases. If the normal axis is rotated out of the null plane in the opposite direction, the opposite occurs, i.e., the wave which increased before now decreases in amplitude while the OD wave increases in amplitude.

The percent increase or decrease in magnitude of the OD waves for various bar orientations is shown in Fig. 4. As noted in this figure, the angular orientation of the bar can be determined by measuring the magnitude and sign of the asymmetry in the OD waves.

Similar amplitude asymmetries were found to exist when the power levels of the OD waves were decreased to near threshold values.

To determine how the polarization of the OD waves changes when the amplitude asymmetries occur, the following experiment, as illustrated in Fig. 2a, is carried out. The polarization of the OD waves is measured from the output of mirror No. 3, while their intensities are measured from the output of mirror No. 2. As before, the opposing fields are applied supporting bidirectional operation, and the bar is placed in the cavity with its normal axis in the null plane ($\alpha = 0$). The polarization of both waves is found to be slightly elliptical. As the bar is rotated to $\alpha = 2°$, the main polarization components of the OD waves are rotated approximately 6° away from their

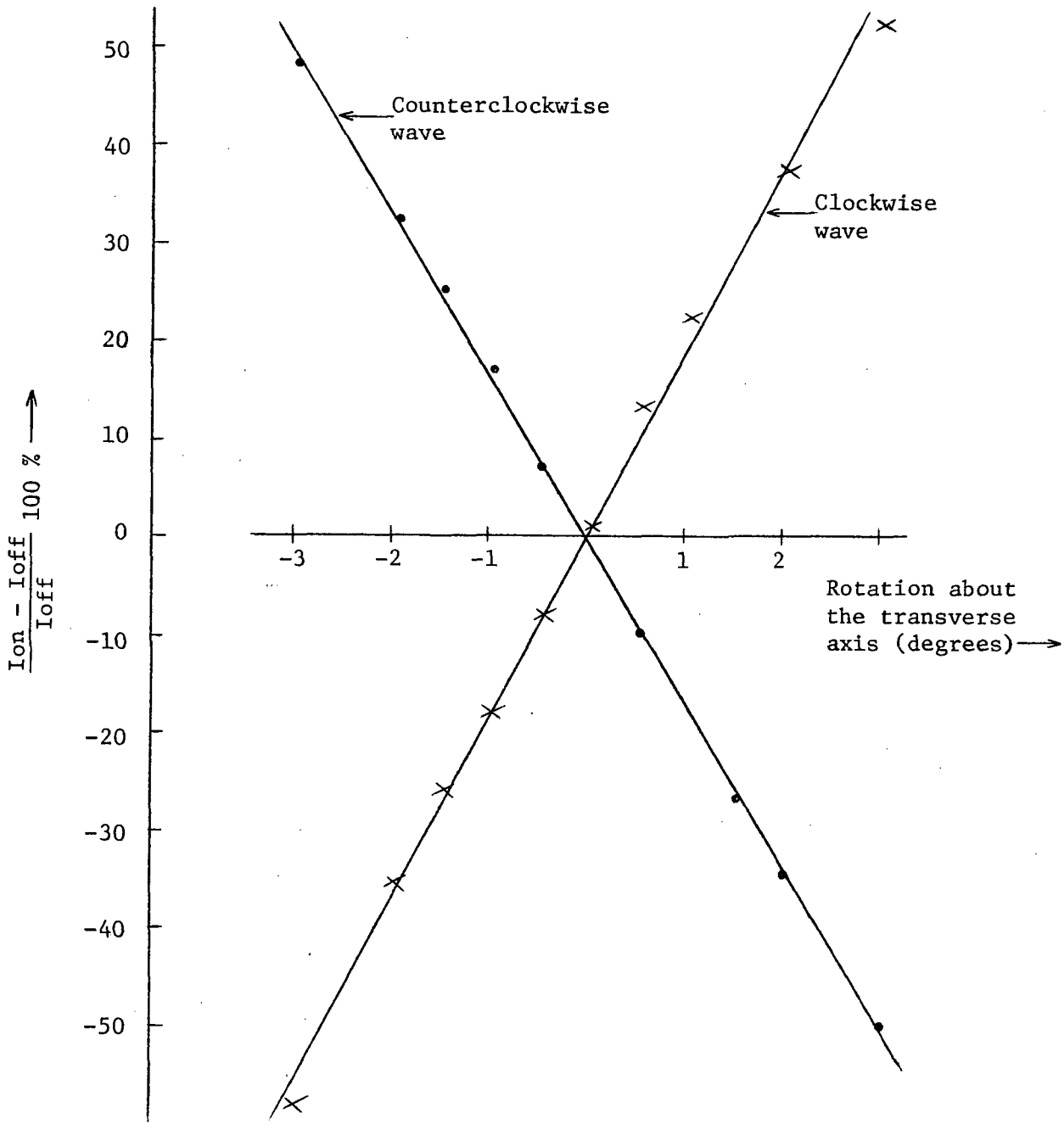

Fig. 4. Percent increase and decrease in the intensity of the OD waves for various values of α, that is, for various bar orientations about the transverse axis when the differential field of 160 gauss is applied. The straight lines are least square fits to data (taken at position of maximum sensitivity).

null plane values, while the amplitudes of both waves decrease equally. The differential field is then applied. The main polarization component of the clockwise wave rotates approximately 1° back toward its null plane value, while the wave amplitude increases. The counterclockwise wave, which decreases in amplitude, has its main polarization component rotated about 1° further from its null plane value. If the bar is, however, rotated to $\alpha = -2°$, the opposite occurs as the differential field is applied, i.e., the counterclockwise wave, which now increases in amplitude, has its main polarization component rotated back toward its null plane value, while the clockwise wave, which now decreases in amplitude, has its main polarization component rotated still further from its null plane value. Thus a polarization asymmetry is found to occur simultaneously with the amplitude asymmetry.

In the above experiments the OD traveling waves were found to be elliptically polarized. To determine the phase difference between the $\hat{x}$ and $\hat{y}$ field components (ψ), the above experiment was repeated. The amplitudes of the major component of polarization, the minor component of polarization, and the angle (ξ) between the major polarization component and the $\hat{x}$ field component (without the bar in the cavity and without magnetic fields applied) were measured for each OD wave. This was accomplished by allowing the output from mirrors No. 1 and No. 2 to pass through a polarizer and then into a detector (see Fig. 1). From this information the phase ψ between the $\hat{x}$ and $\hat{y}$ field components is found by solving the transcendental equations given by Born and

Wolf.[52] With the bar in the cavity (as shown in Fig. 3) and balanced fields, the results for one direction are shown in Table 1. For the

Table 1. Determination of phase angle ψ between the $\hat{x}$ and $\hat{y}$ field components for a balanced magnetic field.

α (Degrees)	ξ (Degrees)	Amplitude of Major Polarization Component (Arbitrary Units)	Amplitude of Minor Polarization Component (Arbitrary Units)	ψ (Degrees)
0	1.5	1.6	.04	40°
3	9	1.15	.045	14°
-3	-10	1.2	.053	194°

OD directed wave we obtain approximately the same results. For a given α, i.e., $\alpha = 0,3,-3$ degrees, the phase angle ψ is found to vary for both directions as the differential field is applied. Due to measurement error it was difficult to determine the amount of this angular variation; however, it appeared to be less than two degrees for each value of α.

The variations in the polarization of the OD waves indicated in Table 1 are in agreement with the changes in the polarization of the OD waves found by Burrell,[53] et al. The change in ψ as α varies

---

[52] M. Born and E. Wolf, *Principles of Optics*, Pergamon Press, 1965, p. 27.

[53] G. J. Burrell, T. S. Moss and A. Hetherington, "Beats Produced by Negative Faraday Effect in Infrared Ring Lasers," *Infrared Physics*, Vol. 8, 1968, pp. 199-208.

from 3 degrees to -3 degrees is also predicted by Troshin,[54] et al., using the Poincaré sphere method of analysis.

The results of the above experiments are summarized as follows. With the laser operating in twelve to fifteen free-running modes, the fields are balanced; we find that as the bar is rotated about the transverse axis such that $\alpha \neq 0$, the amplitudes of the OD waves decrease. Such behavior is predicted by the threshold population requirement in Eq. 62. Then, as the differential field is applied, we find that for $\alpha \neq 0$ the asymmetries occur. This behavior is also in agreement with theoretical predictions as in Eq. 63.

We also find polarization asymmetries to occur between the OD waves, as one would expect from the discussion of the reactive balance equations.

2.5. Related Experiments

To more thoroughly understand the polarization asymmetries and the role the three-mirror cavity plays in the asymmetric effects, several additional experiments have been performed. We will now explain a few of the more significant of these experiments.

The polarization of the waves in the ring laser is determined by several factors, the Brewster windows, resonance conditions in the

---

[54] B. I. Troshin and S. N. Bagaev, "Use of the Poincaré Sphere Method for the Analysis of the Polarization Characteristics of a Laser with an Anisotropic Element," *Optics and Spectroscopy*, Vol. 23, No. 5, November 1967, pp. 424-425.

three-mirror ring cavity, the quartz bar, and the magnetic field effects upon the gain atoms. Polarization effects occur due to the Brewster windows because they have a minimum reflection loss for only one linear polarization.

As we have discussed in chapter I an empty three-mirror cavity can only support waves having one of two polarizations -- waves having a polarization perpendicular to the plane of the ring, and waves having a polarization in the plane of the ring. This is illustrated in the following experiment. Without the bar in the cavity, the amplifier tube is positioned so that the Brewster windows have minimum reflection loss for waves with polarization perpendicular to the plane of the ring. The current to the electromagnets is turned off causing unidirectional operation. When the tube is rotated about its axis away from this position by as little as ±4°, the amplitude of either OD wave is greatly reduced, and its polarization, while remaining essentially linear, is rotated by approximately ±2°. For tube rotations of ±6°, both OD waves are completely extinguished. Similar results were obtained by Bagaev,[55] et al. In a cavity with an even number of mirrors, the restriction on the allowed polarization is lifted since the resonant cavity length for both polarizations is now the same. For example, we find that in a four-mirror ring cavity, the amplifier tube must be rotated by as much as 20° to cause any significant amplitude changes.

---

[55] S. N. Bagaev, et al., *op. cit.*

There are several sources of polarization effects in the quartz bar. The bar, like the Brewster windows, has a minimum reflection loss for only one polarization. However, the significant property of the bar is its birefringence since the asymmetries disappear when the quartz bar is replaced with an isotropic glass bar. The birefringence of the quartz bar is the source of two types of behavior; one is beam splitting, the other is a change in the polarization. Calculation shows that the magnitude of the beam splitting due to birefringence is about one percent of the average beam diameter. Since this splitting is so small, it is doubtful that it contributes to the asymmetric effect. Regarding polarization changes, a linearly polarized wave entering the quartz bar will, in general, exit with an elliptical polarization. As the bar is rotated in one angular direction about the transverse axis, we find experimentally that a wave "A" traveling on a single pass through the bar (as shown in Fig. 3) has its main polarization component rotated in a clockwise manner, "viewed" face on into the propagation direction of "A". For the same bar rotation, wave "B" traveling through the bar in the opposite direction has its main polarization component rotated in a counterclockwise manner, "viewed" face on into the propagation direction of "B". Thus, as the bar is rotated about the transverse axis, the main polarization components of waves traveling through it in opposite directions are rotated in a nonreciprocal manner. However, if the light travels on a single pass through a three-mirror/quartz bar combination (such as in Fig. 5a) then, when the bar is rotated as above, the main polarization components

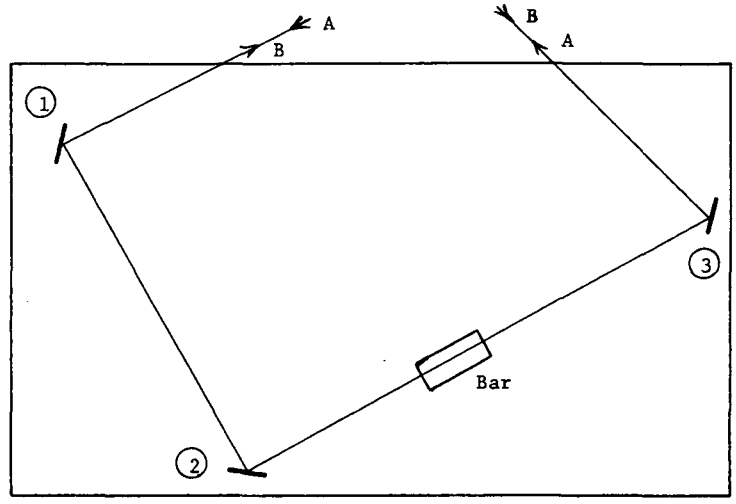

(a)

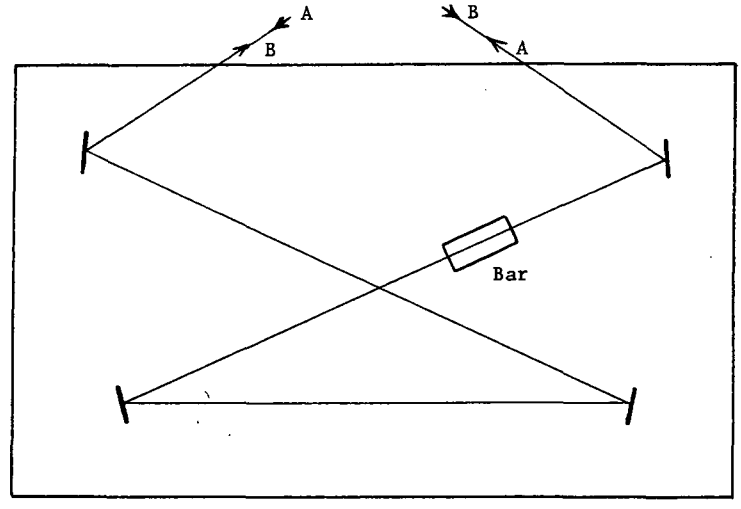

(b)

Fig. 5. Experimental arrangement used to determine the polarization rotation characteristics of light passing through the quartz bar as the bar is rotated about the transverse axis (see Fig. 3):

a. In a three mirror arrangement.

b. In a four mirror arrangement.

of the OD waves are rotated in a reciprocal manner. This is shown in the experiment which is illustrated in Fig. 5a. The OD waves "A" and "B" enter the three-mirror/quartz bar combination with linear polarization perpendicular to the plane formed by the three mirrors. Wave "A" travels past mirrors No. 1 and No. 2 and arrives at the bar with a polarization still perpendicular to the plane formed by the three mirrors. As the wave passes through the bar, its polarization becomes elliptical. When the bar is rotated about the transverse axis in one angular direction, the main polarization component of wave "A" is rotated in a counterclockwise direction. This rotation becomes clockwise upon reflection from mirror No. 3 and the wave exits the arrangement with polarization rotated clockwise. Wave "B" travels past mirror No. 3 and also arrives at the bar with a polarization perpendicular to the plane formed by the three mirrors, and upon passing through the bar, its polarization becomes elliptical. When the bar is rotated in the same manner as above, the main polarization component of wave "B" receives a clockwise rotation. Mirror No. 2 changes this to a counterclockwise rotation while mirror No. 1 changes it back to clockwise rotation, so wave "B" also exits the arrangement with polarization rotated clockwise. Thus, for bar rotations about the transverse axis, the main polarization components of the OD waves are rotated in a reciprocal manner when traveling on a single pass through a three-mirror/quartz bar combination. On the other hand, with an even number of mirrors, such as the four-mirror/quartz bar combination shown in Fig. 5b, this is not the case. We now find for the same bar rotations

that the OD waves are rotated in a nonreciprocal manner. The same reciprocal/nonreciprocal behavior was observed when the quartz bar was replaced with, respectively, a Faraday rotator and a quarter-wave plate at various orientations.

To observe how the axial magnetic field in the active medium influences the polarization of waves passing through it, the following experiment was performed. Linearly polarized light from a three-mode laser (Spectra Physics 130 C) was passed through the discharge of the active medium. When the axial field is increased in one direction from 0 to 130 gauss, the polarization becomes elliptical with the main polarization component receiving a clockwise rotation of approximately 0.5°. If the light is passed through the discharge in the opposite direction and the experiment repeated, the main polarization component receives a counterclockwise rotation of approximately 0.5°. Thus, the main polarization components of OD waves are rotated in a nonreciprocal manner. We have been unable to find magnetic field experiments similar to the above at λ = 6328 Å in the literature; however, related work is reported in several articles.[56-59]

If the three-mirror/bar combination and the active medium in the presence of an axial magnetic field are combined as in Fig. 2a, then, on a single pass, different polarization changes occur depending

---

[56] M. Sargent, III, et al., *op. cit.*

[57] R. G. Buser, et al., *op. cit.*

[58] C. V. Heer, et al., *op. cit.*

[59] G. J. Burrell, et al., *op. cit.*

upon which direction the waves are traversing the cavity.

It is difficult to draw such a single pass analogy for the amplitudes of the OD waves. However, in terms of the theoretical analysis such a combination of elements are necessary to set up an asymmetric threshold polarization. If such a combination were not used, for example, if we had used the same experimental arrangement in a four-mirror cavity, then the OD waves in first order would vary the same from a threshold population standpoint, and consequently should have equal amplitudes in the operating laser. It is important to note that we have been unable to observe asymmetric amplitude effects or asymmetric polarization changes between the OD waves in a four-mirror ring cavity.

2.6. Rotations About the Longitudinal and Normal Axes

We would like to know how the asymmetries vary for rotations of the bar about the other two axes -- the longitudinal axis and the normal axis.

We find that the sensitivity (percent difference in intensity versus angle of rotation) of the asymmetric effect depends upon the angular position of the bar about the longitudinal axis. The maximum sensitivity occurs at one particular angular position (θ_p) of the transverse axis (see Fig. 3). At this angular position the light is incident on the bar at approximately the Brewster angle of quartz. The data in Fig. 6 show the maximum sensitivity to be approximately 17 percent/degree. It is not understood why the sensitivity decreases

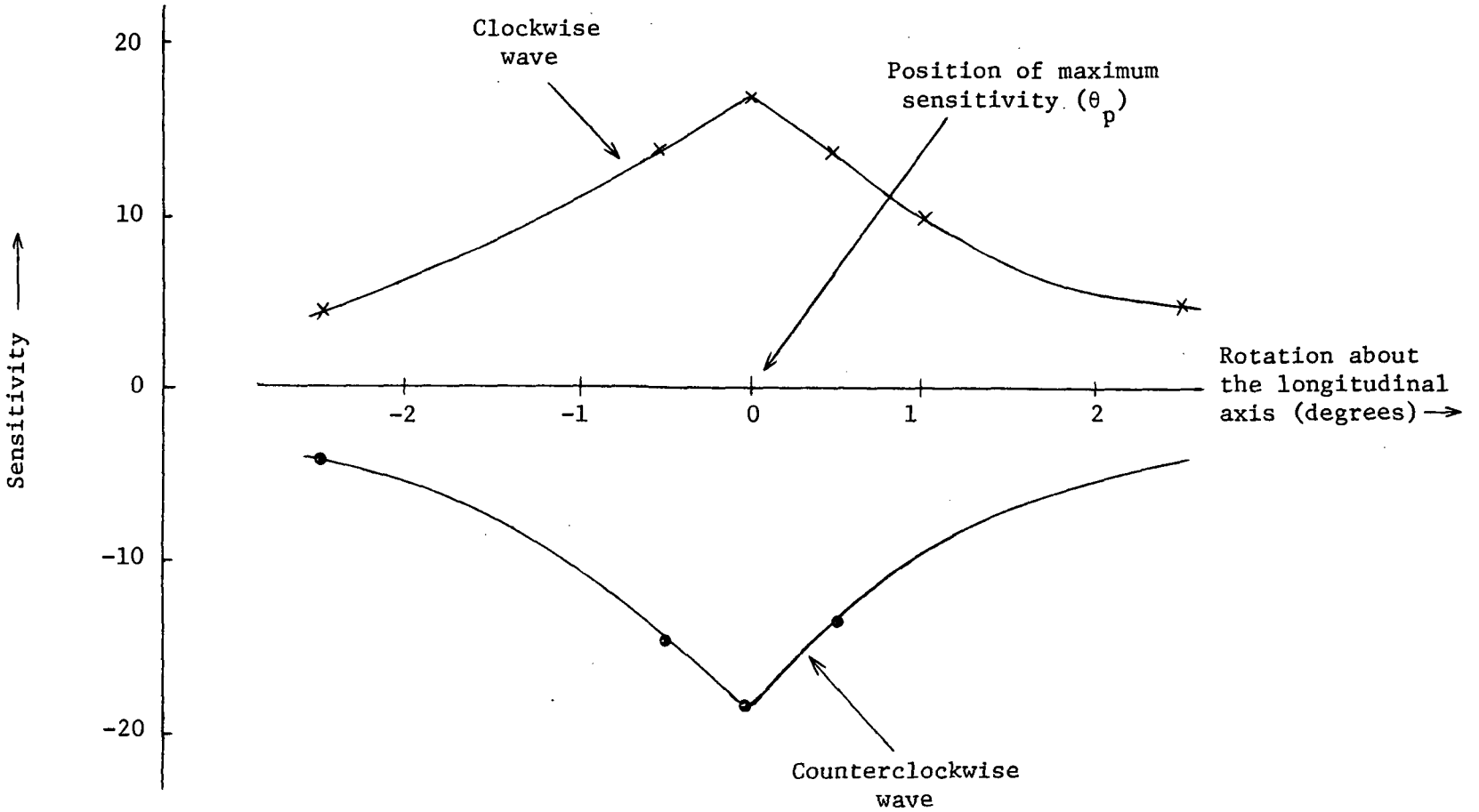

Fig. 6. Sensitivity (percent intensity change/degree rotation about the transverse axis) for various bar orientations about the longitudinal axis.

when the bar is rotated away from θ_p. One possible reason, however, is the occurrence of optical activity for bar rotations other than θ_p. The effects of optical activity, which have not been considered in the theory, reduce to zero for bar orientations such that θ is near the Brewster angle of quartz, i.e., near θ_p, and as one rotates the bar about the longitudinal axis away from θ_p, the effects of optical activity will be present.[60] Optical activity has a behavior different from birefringence in that it always causes the polarization of the two OD waves to be rotated in a reciprocal manner.[61] From the results of our discussion of single-pass measurements and the theoretical predictions, we can see that in a three-mirror cavity such behavior would not lead to the observed amplitude asymmetries. The combined effects of both optical activity and birefringence might, therefore, be causing a reduction in the magnitude of the amplitude asymmetries. Another possibility for this behavior is the fact that as the bar is rotated, the optical length through the bar changes slightly which could lead to a drop in the sensitivity in some unexplained manner. These unanswered questions are topics for future research.

While experimentally determining the characteristics of the asymmetric effect, the bar's c-axis had been positioned in the null plane. To investigate how the position of the c-axis influences the

---

[60] J. F. Nye, *Physical Properties of Crystals*, Clarendon Press, Oxford, 1957, p. 263.

[61] E. U. Condon, "Theories of Optical Rotatory Power," *Reviews of Modern Physics*, Vol. 9, No. 4, October 1937, pp. 432-457.

asymmetric effect, the bar was rotated about the normal axis so that the c-axis was a few degrees out of the null plane (see Fig. 3). We found that the asymmetric null (angular position of the bar about the transverse axis at which no differential amplitude changes occur) is displaced away from the null plane, as shown in Fig. 7. Thus, one can measure the angular position of the c-axis by locating the position of the asymmetric null.

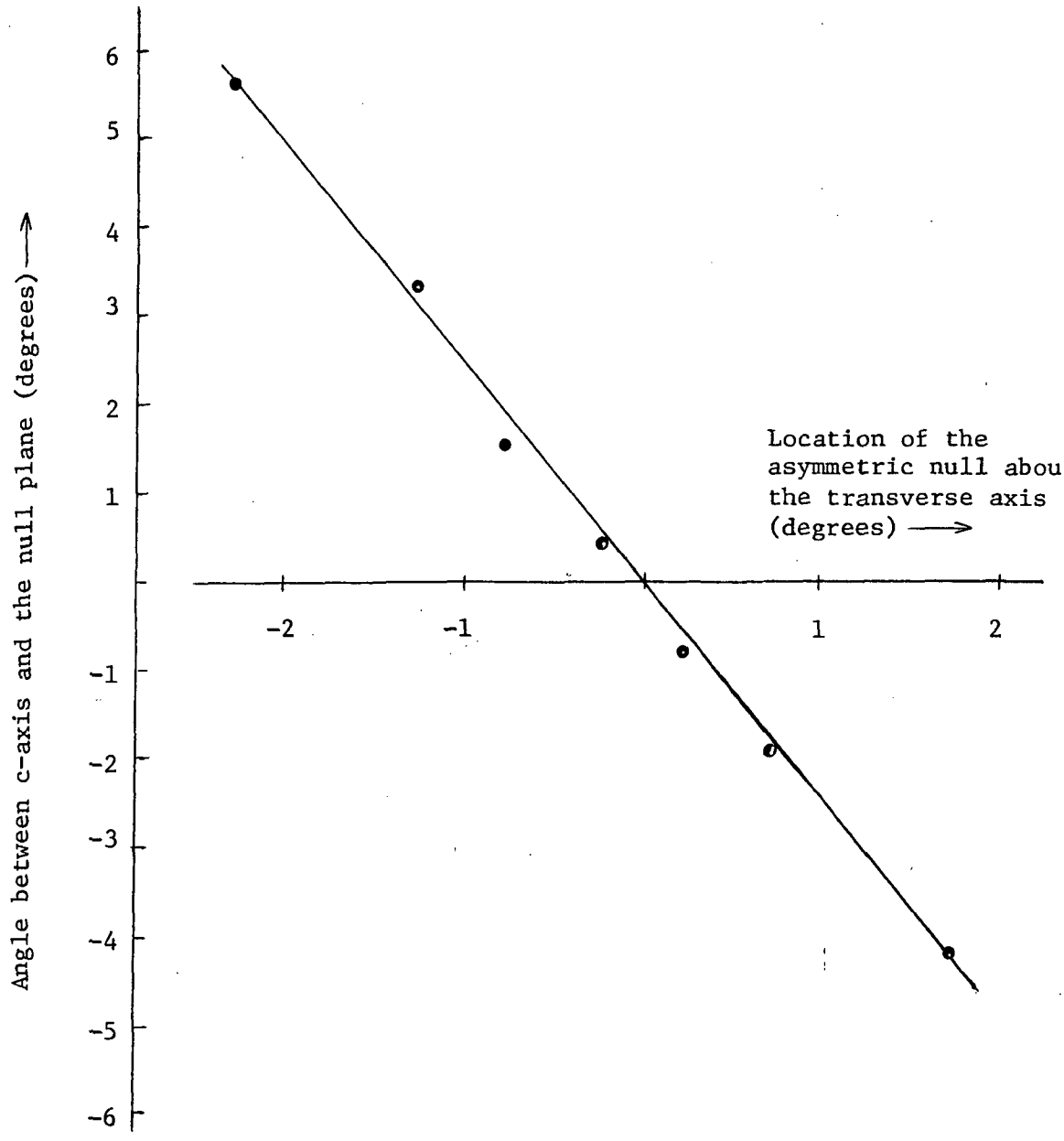

Fig. 7. Shift in the position of the asymmetric null as the bar's c-axis is rotated about the normal axis out of the null plane. The straight line is a least square fit to the data.

III. CONCLUSIONS

We have attempted theoretically to describe a phenomena taking place in a ring laser system. This system is characterized by many parameters, all of which influence its behavior to some degree. The active medium, which drives the electromagnetic fields propagating in each direction, is the source of several of these parameters. The electromagnets cause axial magnetic field effects to occur in the active medium. Since the laser operates well above threshold, other effects result such as competition between modes of the same direction, between modes of the opposite direction, and saturation. Besides the active medium additional parameters effecting the system occur in the cavity, i.e., the Brewster windows cause anisotropic losses to exist, particular resonance conditions result from the three-mirror cavity configuration, and the quartz bar leads to the occurrence of linear birefringence beam splitting and optical activity. A very complicated problem results when all of these effects are included in a theoretical model of the system. We have tried a simpler approach to the problem while still trying to account for the phenomena.

Our method was to use a first order perturbation theory in powers of the electric field to describe the active medium while including magnetic field effects upon the gain atoms. In modeling the quartz bar the effects of optical activity and beam splitting were not included since they are very small.

Our first order theory satisfactorily explains the source of the phenomena of amplitude and polarization asymmetries. Specifically, the theory predicts that for balanced opposing magnetic fields applied to the active medium, the amplitude of both OD waves symmetrically decrease as the bar is rotated away from $\alpha = 0$. Such behavior was found to exist in the oscillating laser. As a differential magnetic field was applied, we found that for bar rotations away from $\alpha = 0$, an amplitude asymmetry occurred between the OD waves. The sign of the amplitude asymmetry reversed when the bar was rotated away from $\alpha = 0$ in the opposite direction. This behavior was also predicted using the first order theory.

The source of these asymmetries was found from the theory to arise from the different optical properties exhibited by the cavity elements for the two propagation directions. That is, the combination of a differential magnetic field in the active medium and a birefringent bar placed in the three-mirror cavity "looks" different for the two OD traveling waves. In particular, the theory shows that as the bar is rotated the resulting variation in χ_{xy} is the important parameter in causing the amplitude changes.

Since the effects of saturation and competition between modes are not predicted in our theory, we cannot theoretically determine how important they are in determining the observed asymmetries. However, experimentally we found that the asymmetric amplitude effects occurred not only under saturation conditions but also when the laser was operated at near threshold power levels. Consequently, we are led to be-

lieve the fundamental source of the asymmetries is predicted by the first order theory presented in chapter I, and higher order effects such as competition between modes and saturation are less important.

As was shown in Fig. 4, the percent increase or decrease in the intensity of the asymmetries is quite linear as a function of α. Thus, the angular orientation of the bar can be easily determined by measuring the magnitude and sign of the asymmetry in the OD waves. The sensitivity of angular measurement in our experimental setup is approximately 1 degree per 17 percent intensity asymmetry.

While we have had success in predicting the qualitative behavior of the system, we have not attempted a quantitative understanding of the system. That is, the ultimate sensitivity of the device, and the parameters which are important in obtaining it, have not been studied. Since the first order theory is fundamentally correct, one can now use it to understand more thoroughly the important parameters. Also, the theory, being quite general, can be used to describe other ring laser problems which include either some or all of the effects of anisotropic loss, linear birefringence, and axial magnetic fields in the active medium.

Other optical materials and effects could be a means of improving the ultimate flexibility and sensitivity of the system. For example, we found it difficult to detect angular orientations for bar angles much greater than three degrees because the OD waves were extinguished. Their extinction probably resulted from increased reflection loss at the bar surfaces since the OD waves were no longer in

the plane of incidence. A useful angular orientation detector must not have this limitation. One method to circumvent the problem would be to measure the angular orientation of the bar for rotations about the normal axis. This can be accomplished by measuring the position of the asymmetric null as illustrated in Fig. 7.

Also, as we have noted, optical activity behaves differently from birefringence, and one might utilize a similar system in a four-mirror cavity to study the optical activity in materials which do not exhibit linear birefringence. These are topics for future study.

DISTRIBUTION LIST

ACTIVITIES AT WRIGHT-PATTERSON AIR FORCE BASE	No. of Copies
AVN	1
AVTL	1
AVWW	1
AVTA	3

OTHER DEPARTMENT OF DEFENSE ACTIVITIES

Air Force

Air University Library Maxwell Air Force Base Alabama 36112	1
AFCRL (CRR-CSA) Att: Mr. Charles Ellis, Jr. L. G. Hanscom Field Bedford, Massachusetts 01731	1
BSD (BSYDF) Attn: Captain Hyslop Norton Air Force Base California 92409	1
RADC (EMATE) Attn: Mr. H. Chiosa Griffiss Air Force Base New York 13440	1

Navy

Chief, Bureau of Ships Attn: Mr. C. C. Walker Department of the Navy Room 3337 Washington, D. C. 20360	1
Director, Naval Research Laboratory Attn: Mr. H. D. Arnett, Code 5244 Washington, D. C. 20360	1

	No. of Copies
Commanding Officer and Director USNASL, Mr. P. J. Giardano U. S. Naval Base Brooklyn, New York 10001	1
Scientific Officer, Code 427 Office of Naval Research Washington, D. C. 20360	1
Director U. S. Naval Electronics Laboratory San Diego, California 92142	1
Chief, Bureau of Ordnance Department of the Navy, Code RE-9 Washington, D. C.	1
Chief, Bureau of Aeronautics Department of the Navy, Code EL-412.1 Washington, D. C. 20025	1
Mr. Jay Froman Office of Naval Research San Francisco Area Office 50 Fell Street San Francisco, California	1

Army

Commanding General U. S. Army Electronics Command Attn: AMSEL-KL-S (Dr. H. Jacobs) Fort Monmouth, New Jersey 07703	1
Commanding General U. S. Army Electronics Command Attn: AMSEL-KL-TM (Mr. Harold J. Hersh) Fort Monmouth, New Jersey 07703	1
Commander, U. S. Army Materiel Command Harry Diamond Laboratories Attn: H. W. A. Gerlach Connecticut and Van Ness Streets, N. W. Washington, D. C. 20025	1

	No. of Copies
Commander, U. S. Army Missile Command Attn: Mr. W. D. McKnight, ORDXR-RBE Redstone Arsenal, Alabama 35809	1
Commanding Officer U. S. Army Mobile Equipment Research and Development Center Attn: Technical Documents Center Building 315, Vault Fort Belvoir, Virginia 22060	1

OTHER U. S. GOVERNMENT AGENCIES

DDC (TISIA) Cameron Station Alexandria, Virginia 22314	12
National Science Foundation Washington District of Columbia 20550	1
Dr. Royal E. Rostenbach Acting Program Director Engineering Energetics, Engineering Division National Science Foundation Washington, D. C. 20550	1
Advisory Group on Electron Devices Attn: Mr. H. N. Serig 201 Varick Street, 9th Floor New York, New York 10014	4
National Bureau of Standards Attn: Librarian Department of Commerce Washington, D. C. 20025	1
U. S. Atomic Energy Commission Division of Research Attn: Dr. Roy W. Gould Washington, D. C. 20545	1
Library U. S. Department of Commerce Environmental Science Services Administration Boulder Laboratories Boulder, Colorado 80302	1

NONGOVERNMENT INDIVIDUALS AND ORGANIZATIONS	No. of Copies
Amperex Electronic Corporation 230 Duffy Avenue Hicksville, New York 11804	1
Dr. J. Mark Baird 2974 Molly Court Newberry Park, California 91302	1
Dr. Paul Berrett 269 ELB Electrical Engineering Department Brigham Young University Provo, Utah 84601	1
Dr. Vladislav Bevc, L382 Lawrence Radiation Laboratory P. O. Box 808 Livermore, California 94551	1
Dr. Lawrence Bowman Brigham Young University, ELB 174 Provo, Utah 84601	1
Dr. C. Kent Bullock Naval Weapons Center Code 4081 China Lake, California 93555	1
Dr. W. Charles Carr Laser Sciences, Inc. Wooster Street Bethel, Connecticut 06801	1
Dr. Edwin G. Chaffee Litton Industries Electron Tube Division Crossed-Field Devices, Dept. 180 960 Industrial Way San Carlos, California 94070	1
Dr. Su-Min Chou 12305 Village Square Terrace Rockville, Maryland 20852	1
Dr. Douglas A. Christensen 895 Windsor Court Santa Barbara, California 93105	1

	No. of Copies
Dr. John C. Clark 8389 Vereda del Padre Goleta, California 93017	1
Cornell University Electrical Engineering Department Attn: Professor Lester F. Eastman 316 Phillips Hall Ithaca, New York 14850	1
Cornell University School of Electrical Engineering Attn: Dr. Joseph M. Ballantyne Ithaca, New York 14850	1
Dr. Maylin Dittmore 241 Helen Way Livermore, California 94550	1
EIMAC, A Division of Varian Associates Attn: Technical Library 301 Industrial Way San Carlos, California 94070	1
EIMAC, A Division of Varian Associates Attn: Dr. George Caryotakis 301 Industrial Way San Carlos, California 94070	1
Eitel-McCullough, Inc. Attn: Larry Hansen, Manager 1678 Pioneer Road Salt Lake City, Utah	1
General Electric Company Research Laboratories Attn: Dr. T. G. Mihran P. O. Box 1088 Schenectady, New York 12305	1
General Telephone and Electronics Physical Electronics Laboratory Attn: Dr. Louis R. Bloom Miss M. Franc, Documents Custodian 208-20 Willets Point Boulevard Bayside, New York 11361	1 1

	No. of Copies
Dr. Lewis C. Goodrich 181 Harbor Drive, No. 4 Claymont, Delaware 19703	1
Grumman Aerospace Corporation Attn: Mr. Paul H. Savet Research Department, Plant 35 Bethpage, New York 11714	1
Dr. David R. Gunderson Bell Telephone Laboratories 4B301 Holmdel, New Jersey 07733	1
Hughes Aircraft Company Attn: Dr. Donald C. Forster 3011 Malibu Canyon Road Malibu, California 90265	1
Dr. Vern R. Johnson Electrical Engineering Department University of Arizona Tucson, Arizona	1
Dr. Tai-wu Kao Electrical Engineering Department Loyola University of Los Angeles 7101 West 80th Street Los Angeles, California 90045	1
Dr. John H. Keller 7 Duchess Court Newburgh, New York 12550	1
Dr. Kenneth G. Leib, Research Engineer Grumman Aerospace Corporation Plant 35 Bethpage, New York 11714	1
Library of Congress Attn: Mr. Nathan R. Einhorn, Chief Exchange and Gift Division Washington, D. C. 20540	1
Dr. C. H. Ma P. O. Box 3894 University, Mississippi 38677	1

	No. of Copies
Alpheus Smith Laboratory Physics Library Ohio State University 174 West 18th Avenue Columbus, Ohio 94210	1
Raytheon Company Attn: Dr. W. C. Brown Microwave and Power Tube Division Building 1 Foundry Avenue Waltham, Massachusetts 02154	1
RCA Laboratories Attn: Dr. Stanley Bloom Member, Technical Staff Princeton, New Jersey 08540	1
S. F. D. Laboratories Attn: Dr. Farney 800 Rahway Avenue Union, New Jersey 07083	1
Dr. Richard L. Schriever 1365 Fairview Court Livermore, California 94550	1
Dr. Aris Silzars 901 Stony Hill Road Redwood City, California 94061	1
Sperry Rand Corporation Electron Tube Division Attn: Dr. Sutherland Gainesville, Florida 32601	1
Stanford University Plasma Physics Library Institute for Plasma Research Attn: Librarian Via Crespi Stanford, California 94305	1
Dr. Kenneth I. Talbot 582 Dublin Way Sunnyvale, California 94807	1

	No. of Copies
Tulane University Electrical Engineering Department Attn: James A. Cronvich New Orleans, Louisiana 70118	1
University of California Electronics Research Laboratory Attn: Professor J. R. Whinnery Berkeley, California 94704	1
University of California Lawrence Radiation Laboratory Attn: Verle Gilson Building 170C, Room 2597 Box 808 Livermore, California 94551	1
University of California Attn: Professor Glen Wade Santa Barbara, California 93107	1
University of Colorado Department of Electrical Engineering Attn: Professor Russell E. Hayes Boulder, Colorado 80304	1
University of Illinois Department of Electrical Engineering Attn: Professor Paul D. Coleman Urbana, Illinois 61801	1
University of Michigan Electrical Engineering Department Attn: Dr. Joseph Rowe, Chairman Ann Arbor, Michigan 48107	1
University of Utah Gifts and Exchanges Division 242 Marriott Library Salt Lake City, Utah 84112	4
University of Utah Solid Rocket Structural Integrity Information Center 4003 W Merrill Engineering Building Salt Lake City, Utah 84112	1
Utah Engineering Experiment Station Attn: Dr. Robert G. Larsen University of Utah 207 Mines Building Salt Lake City, Utah 84112	1

	No. of Copies
Varian Associates, Inc. Attn: Technical Library 611 Hansen Way Palo Alto, California 94303	1
Watkins-Johnson Company Attn: Dr. O. T. Purl, Vice President 3333 Hillview Avenue Stanford Industrial Park Palo Alto, California 94304	1
Dr. David C. Watson Electromagnetic Systems Laboratory 495 Java Drive Sunnyvale, California 94086	1
Westinghouse Electric Corporation Defense and Space Center Aerospace Division Attn: H. W. Cooper, MS 129 Friendship International Airport Baltimore, Maryland 21203	1
Zenith Radio Corporation Attn: Dr. Robert Adler, Director of Research 6001 West Dickens Avenue Chicago, Illinois 60639	1
Dr. Larry L. Campbell 11627 Vantage Hill Road Reston, Virginia 22070	1